


 Cite this: *RSC Adv.*, 2023, **13**, 25054

Microwave-assisted chemoselective synthesis and photophysical properties of 2-aryldazo-biphenyl-4-carboxamides from hydrazonals†

 Abdulrahman M. Alazemi,¹ ^{*a} Kamal M. Dawood,² ^{*b} Hamad M. Al-Matar ^a and Wael M. Tohamy ^{ac}

The reaction of 3-oxo-2-arylhydrazonopropanals with acetoacetanilide in an equimolar ratio, under DBU/1,4-dioxane/microwave irradiation reaction conditions, resulted in chemoselective formation of 4-aryldazo-5-hydroxy-benzamide derivatives. The structures of the obtained biphenyl-4-carboxamides were characterized by several spectroscopic techniques including IR, ¹H- and ¹³C-NMR, MS and HRMS, and X-ray single crystals of three examples. The photophysical properties of the new products were also evaluated, with a particular focus on their absorption and emission spectra, which provided valuable information regarding their optical properties. The new compounds emitted 513–549 nm green fluorescence in acetone solution under UV irradiation.

 Received 8th July 2023
 Accepted 7th August 2023

DOI: 10.1039/d3ra04558g

rsc.li/rsc-advances

1. Introduction

Salicylanilides (2-hydroxy-*N*-phenylbenzamides) have attracted substantial research interest from the field of medicinal chemistry owing to their exceptional bioactivities. They exhibit anti-inflammatory, antibacterial, antifungal activities,^{1–9} are antiviral agents against various viral pathogens such as coronaviruses (MERS-CoV & SARS-CoV), West Nile virus (WNV), Hepatitis-C virus (HCV), Japanese encephalitis virus (JEV), human rhinovirus (HRV), dengue virus (DENV), yellow fever virus (YFV)^{10–12} and are used for treatment of tuberculosis.^{13–15}

The Salicylanilide family is useful in veterinary and human medicines. For example, as shown in Fig. 1, *Oxyclozanide*,¹⁶ *Closantel*¹⁷ was discovered to be a powerful antistaphylococcal,^{18–21} *Rafoxanide*²² was successful for the treatment of *F. hepatica* infection in cattle and sheep, and *Niclosamide*, was approved by FDA as an anthelmintic drug,^{23,24} highly potent for treatment of COVID-19 and SARS-CoV-2 (ref. 25–28) and has high anti-cancer activity.^{29–32}

The classical synthesis of salicylanilides was achieved by condensing the appropriate salicylic acid derivatives with aromatic amines in the presence of dehydrating agents such as

phosphorus oxychloride,³³ phosphorus trichloride,^{34–36} carbonyldiimidazole (CDI),³⁷ 1-(3-dimethylamino-propyl)-3-ethylcarbodiimide (EDC),³⁸ thionyl chloride,^{39,40} P₂O₅,⁴¹ or *N,N'*-dicyclohexylcarbodiimide (DCC).⁴² High boiling solvents such as xylene, chlorobenzene, or toluene were used or solvent-free conditions were used. These processes were fairly difficult and lengthy due to the low reactivity of the carboxylic acids.⁴³ Aminolysis of phenyl salicylate in chlorobenzene or xylene was also used when the solvent offered a significant challenge in the separation process of the product.^{4,13,36} Thus, we concluded that these procedures had many obstacles, such as complicated operations, expensive reagents, low productivity and long reaction times. On the other hand, aryl azobenzene systems were of valuable importance in various fields, such as dye industries,⁴⁴ liquid crystals,^{45,46} material science,^{47,48} chemosensors,^{49,50} polymers,⁵¹ photochemical switches⁵² and pharmaceutical products.^{53–55} Microwave radiation produces a rapid intense heating of polar compounds, resulting in significantly shorter reaction times, high reaction yields and a cleaner technique.

The fundamental advantage of microwave heating is its significant energy savings through its instantaneous “in-core” heating of substances in a selective and homogeneous manner with a significantly shorter response time.^{56–58} The straightforward amidation of carboxylic acids was successfully modified by microwave activation.^{59–65} Therefore, in continuation of our research interest in microwave-assisted organic synthesis,^{66–77} herein we re-investigated our previous work on a supplemental reaction of 3-oxo-2-arylhydrazonopropanals **1** with acetoacetanilide **2**,⁶⁸ by optimization of reaction conditions (components' molar ratios, solvents, bases and activation modes) towards chemoselective construction of the 2-(aryldazo)-5-hydroxy-*N*-

^aChemistry Department, Faculty of Science, University of Kuwait, P.O. Box 5969, Safat 13060, Kuwait. E-mail: a.alazmi@ku.edu.kw; Fax: +965 24816482

^bDepartment of Chemistry, Faculty of Science, Cairo University, Giza 12613, Egypt. E-mail: kmdawood@sci.cu.edu.eg; Fax: +202 35727556

^cOrganometallic and Organometalloid Chemistry Department, National Research Centre, Cairo, Egypt

 † Electronic supplementary information (ESI) available. CCDC 2270147–2270149: crystallographic data for compounds **3f** (2270147), **3h** (2270148) and **3n** (2270149). For ESI and crystallographic data in CIF or other electronic format see DOI: <https://doi.org/10.1039/d3ra04558g>

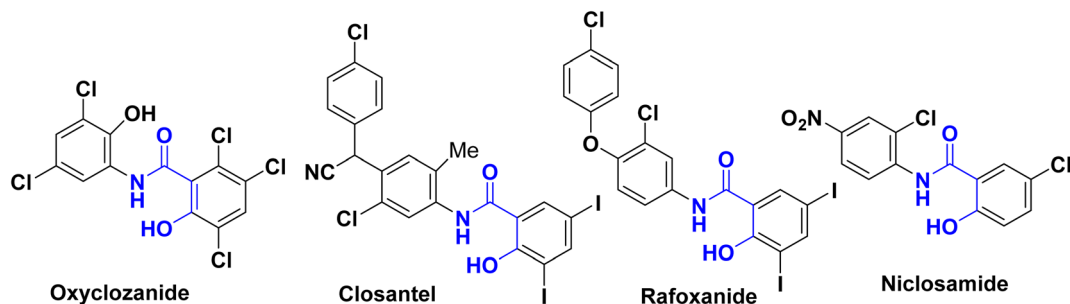
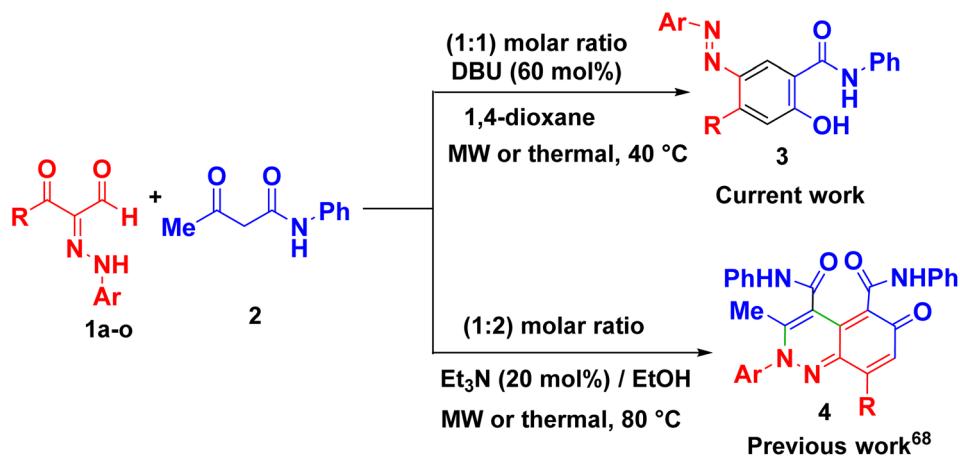



Fig. 1 Examples of bioactive salicylanilides.

Scheme 1 Current and previous work on reaction of 3-oxo-2-arylhydrazonopropanals **1** with acetoacetanilide **2**.

phenyl-[1,1'-biphenyl]-4-carboxamide derivatives **3** instead of the cinnoline derivatives **4** (Scheme 1) and the photophysical properties of the obtained biphenyl-4-carboxamides were evaluated. The structures of the new products were characterized by IR, ¹H- and ¹³C-NMR, MS and HRMS spectral data as well as X-ray single crystallography of selected examples. The photoluminescent spectrum and UV-Vis absorption were also studied.

2. Results and discussion

The key starting substrates 3-oxo-2-arylhydrazonopropanals **1a-o** were prepared following the literature procedures.^{78,79} A representative reaction example was conducted by heating an equimolar ratio of 3-oxo-2-(4-bromophenyl)hydrazonopropanal **1a** and acetoacetanilide **2** under various reaction conditions (different solvents, different bases and different heating modes) as shown in Table 1 and Scheme 2. Thus, the effect of solvents (such as methanol, ethanol, hexane, DMF, chloroform, toluene, 1,4-dioxane) on the reaction between **1a** and **2** using DBU (60 mol%) as an organic base, under thermal heating and microwave irradiation at 40 °C was carefully studied and the reaction path was checked by TLC. Conducting the reaction in methanol under thermal heating for 2 h afforded a mixture of the 4-bromophenylazo-5-hydroxy-benzamide derivative **3a** and the 2,6-dihydrocinnoline-4,5-dicarboxamide **4a** in 50% and 40% yields, respectively, compared with 65% and 28% yields after for

3 min of microwave irradiation (entry 1, Table 1). Repeating the same reaction using ethanol, hexane, DMF, chloroform, toluene, 1,4-dioxane, as reaction solvents, led to the formation of a mixture of **3a** and **4a** in 45–60% and 36–42%, respectively, under thermal condition compared with 52–68% (**3a**) and 25–32% (**4a**) yields under microwave condition (entries 2–6, Table 1). However, 1,4-dioxane was found to be the proper reaction solvent (at 40 °C and DBU (0.6 mmol)) where it exclusively directed the reaction towards the formation of **3e** chemoselectively (95% yield) under microwave irradiation compared with a mixture of **3a** (in 84% yield) and **4a** (in 10% yield), respectively, under thermal heating (entry 7, Table 1). When the same reaction was repeated under typical reaction factors but at room temperature a mixture of the products **3a** and **4a** were obtained in 48% and 40% yields under conventional condition and in 60% and 25% yields under microwave, respectively (entry 8, Table 1). Then, the same reaction condition was repeated using different concentrations of DBU (50 mol% and 80 mol%), at 40 °C, interestingly only **3a** was chemoselectively isolated in 88 and 90% yields, respectively, under microwave conditions compared with about 80% (**3a**) and 14% (**4a**) under thermal heating (entries 9 and 10, Table 1).

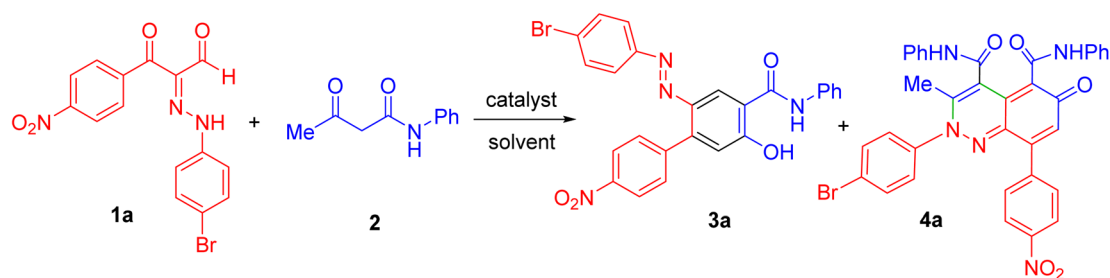
Changing the catalytic base also affected the chemoselectivity, where replacing DBU with pyridine and DABCO (60 mol% all), in dioxane at 40 °C resulted in the formation of a mixture, in all cases, of the carboxamide **3a** and cinnoline **4a**



Table 1 Optimization of the annulation reaction condition of **1a** with **2**^a

Entry	Base (mol%)	Solvent	Temp. (°C)	Thermal (2 h)		MW (3 min)	
				Yield ^b		Yield ^b	
				3a	4a	3a	4a
1	DBU (60%)	Methanol	40	50	40	65	28
2	DBU (60%)	Ethanol	40	55	38	67	25
3	DBU (60%)	Hexane	40	45	42	52	32
4	DBU (60%)	DMF	40	60	36	65	25
5	DBU (60%)	Chloroform	40	58	38	68	25
6	DBU (60%)	Toluene	40	50	40	60	28
7	DBU (60%)	1,4 dioxane	40	84	10	95	Trace
8	DBU (60%)	1,4 dioxane	rt	48	40	60	25
9	DBU (50%)	1,4 dioxane	40	80	14	88	Trace
10	DBU (80%)	1,4 dioxane	40	82	14	90	Trace
11	Pyridine (60%)	1,4 dioxane	40	33	54	42	45
12	DABCO (60%)	1,4 dioxane	40	38	50	45	42
13	Et ₃ N (60%)	1,4 dioxane	40	Trace	25	Trace	34
14	KOH (60%)	1,4 dioxane	40	48	40	55	35
15	Cs ₂ CO ₃ (60%)	1,4 dioxane	40	52	30	68	22
16	Na ₂ CO ₃ (60%)	1,4 dioxane	40	50	40	60	28
17	NaHCO ₃ (60%)	1,4 dioxane	40	65	20	72	18

^a Reaction condition: **1a** (0.5 mmol), acetoacetanilide (0.5 mmol), solvent (6 mL) and base (50–80 mol%), (6 mL), at 40 °C for 2 h, microwave irradiations at 40 °C (200 W) for 3 min. ^b Isolated yields of **3a** and **4a**.

Scheme 2 Annulation of the arylhydrazonopropanal **1a** with acetoacetanilide **2**.

in yields varied between 33–48% and 40–54% under thermal heating and between 42–55% and 35–45% under microwave condition, respectively (entries 11, 12, Table 1). Using Et₃N instead of DBU (60 mol%) in dioxane at 40 °C led to the selective formation of the cinnoline derivative **4a** in low yields; 25% and 34% under thermal and microwave conditions, respectively (entries 13, Table 1). Some inorganic bases were also tested for this reaction by applying the same condition as above. Thence, KOH, Cs₂CO₃, Na₂CO₃ and NaHCO₃ (60 mol% each) was employed separately where in all cases a mixture of the two products **3a** and **4a** were obtained in variable yields; 48–65% (**3a**) and 30–40% (**4a**), respectively under a thermal mode but in 55–72% (**3a**) and 18–35% (**4a**) under microwave mode, respectively (entries 14–17, Table 1). Therefore, the highest chemoselectivity towards the formation of the pure **3a** structure was established using the reaction system; **1a**/2/base/solvent/temperature/heating mode; 1 mmol/1 mmol/0.6 mmol DBU/1,4-dioxane/40 °C/microwave irradiation.

It was concluded that the outcomes of microwave irradiation were established by high productivity and chemoselectivity compared with thermal heating mode. The chemical constitution of the reaction product **3a** was confirmed from its micro-analytical and all possible spectroscopic analyses (IR, ¹H- and ¹³C-NMR, MS and HRMS). Spectral data and the melting point of structure of **4a** were typical of that previously published by our group.⁶⁸ Microwave works faster in polar solvents where it is well known that polar solvents absorb microwave energy faster and convert it into heat leading to bulk heating and simultaneously elevating the reaction temperature, in contrast with thermal conductive heating mode.

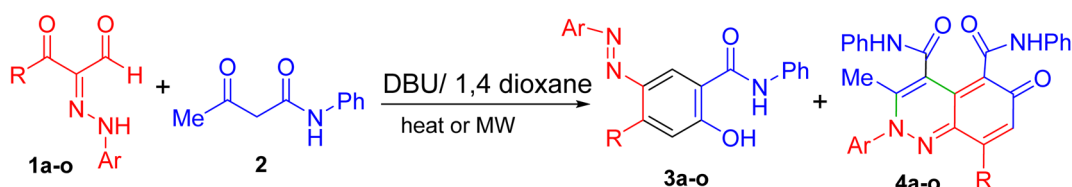
In the following, the best-optimized condition above was applied in the assembly of a library of 5-aryloxy-2-hydroxybenzamides **3a-o** as described in Table 2 and Scheme 3. Thus, conducting the reaction of various 3-oxo-2-arylhyaazonopropanal **1a-o** and acetoacetanilide **2** and molar ratios of the components and reaction conditions were as follows; **1a-o**/2/base/solvent/temperature; 0.5 mmol/0.5 mmol/



Table 2 DBU-catalyzed tandem annulation of arylhydrazonopropanals **1a–o** with acetoacetanilide **2** under conventional and microwave conditions^a

Entry	Products	R	Ar	Thermal (2 h)		MW (3 min)	
				3	4	3	4
1	3a/4a	4-NO ₂ C ₆ H ₄	4-BrC ₆ H ₄	84	10	95	Trace
2	3b/4b	4-NO ₂ C ₆ H ₄	4-ClC ₆ H ₄	80	13	93	Trace
3	3c/4c	4-NO ₂ C ₆ H ₄	3-ClC ₆ H ₄	78	16	90	Trace
4	3d/4d	4-NO ₂ C ₆ H ₄	C ₆ H ₅	72	20	83	10
5	3e/4e	4-ClC ₆ H ₄	C ₆ H ₅	62	28	70	22
6	3f/4f	4-ClC ₆ H ₄	4-BrC ₆ H ₄	74	18	86	8
7	3g/4g	4-BrC ₆ H ₄	4-ClC ₆ H ₄	66	25	75	16
8	3h/4h	4-BrC ₆ H ₄	4-BrC ₆ H ₄	67	25	75	18
9	3i/4i	4-FC ₆ H ₄	4-ClC ₆ H ₄	75	18	88	Trace
10	3j/4j	4-FC ₆ H ₄	4-BrC ₆ H ₄	76	18	88	Trace
11	3k/4k	4-OMeC ₆ H ₄	4-BrC ₆ H ₄	52	38	60	28
12	3l/4l	4-OMeC ₆ H ₄	<i>o</i> -NO ₂ C ₆ H ₄	55	35	64	24
13	3m/4m	C ₆ H ₅	4-ClC ₆ H ₄	62	27	70	20
14	3n/4n	C ₆ H ₅	4-BrC ₆ H ₄	60	30	70	18
15	3o/4o	C ₆ H ₅	<i>o</i> -NO ₂ C ₆ H ₄	70	20	83	10

^a Reaction condition: **1a–o** (0.5 mmol), acetoacetanilide **2** (0.5 mmol), DBU (0.3 mmol) in 1,4-dioxane (6 mL), at 40 °C for 2 h (thermal heating), and 40 °C (200 W) for 3 min (microwave irradiation). ^b Isolated yields of **3** and **4**.

**Scheme 3** Annulation of arylhydrazonopropanals **1a–o** with acetoacetanilide **2**.

0.3 mmol DBU/1,4-dioxane (6 mL)/40 °C, both under thermal as well as microwave irradiating conditions. Again, heating under microwave conditions led to an increase in the chemoselectivity towards the formation of the products **3a–o** compared with conventional heating, where the yields dramatically enhanced when conventional heating was switched to microwave heating and compounds **3a–c** as well as **3i–j** were obtained as the sole products (entries 1, 2, 3, 9, 10, Table 2). In these examples, the R groups of the respective hydrazonal substrates **1** had highly electron-withdrawing substituents (NO₂ or F). In the other examples, microwave irradiation of compounds **1** having groups other than NO₂ or F resulted in the formation of a mixture of compounds **3** and **4** mostly in 8 : 1 ratios of total >90% yields. In contrast, conventional heating led, in all cases, to the production of a mixture of **3a–c** and **4a–c** in 8 : 1 ratios of total >90% yields. The presence of the electron-donating (MeO) group led to the least chemoselectivity, where products **3** and **4** were obtained in almost 2 : 1 ratio under both thermal as well as microwave conditions (entries 11, 12, Table 2). Thus, chemoselectivity was encountered only under microwave for the hydrazonals **1** having highly electron-withdrawing substituents on the R moiety. All structures of the isolated products were thoroughly characterized using spectral analyses as well as X-ray

single crystals of selected compounds (**3f**, **3h** and **3n**) (Fig. 2).⁸⁰ Mechanistically, formation of the 4-aryloxy-5-hydroxybenzamide derivatives **3a–o** and the 2,6-dihydrocinnoline-4,5-dicarboxamides **4a–o** proceeded in a tandem pathway as described in Scheme 4.

2.1. Photophysical studies

The photophysical properties of the synthesized azodye derivatives **3a–o** revealed distinct absorption and emission characteristics. Fig. 3 showed how the substituents (R¹ and R²) in the molecular structure affected the absorption and emission bands. We studied the azodye photophysical behaviors by systematically changing these substituents. Understanding these structure–property correlations allows organic molecules to be used in optoelectronic devices and sensor platforms by changing their optical properties.

All photophysical characteristic data were displayed and applied to determine the maximum wavelength absorption ($\lambda_{\max/abs}$), maximum molar absorptivity (ϵ_{\max}), and maximum wavelength emission ($\lambda_{\max/em}$) for all the azodyes as described in Table 3. The Ultraviolet-Visible (UV-Vis) spectra (Fig. 4a) indicated absorption bands ranging between 444 and 476 nm. Notably, compound **3o** had the largest absorption maxima in



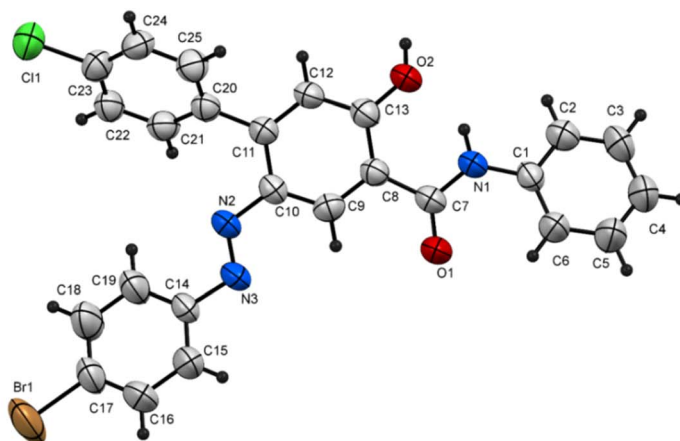
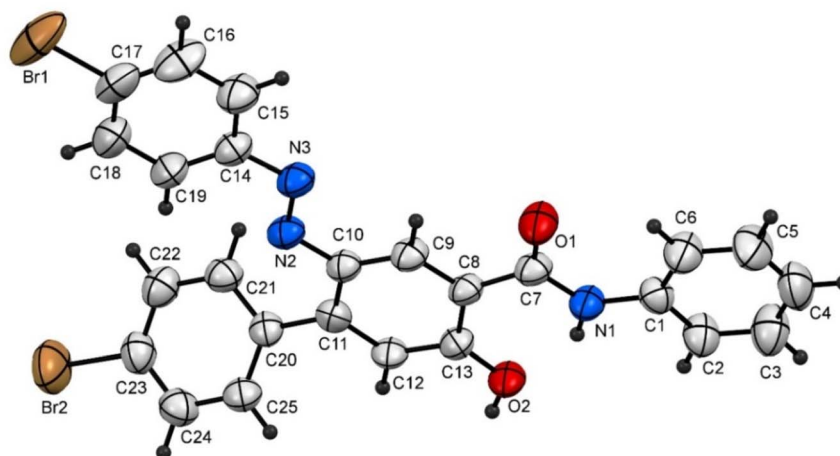
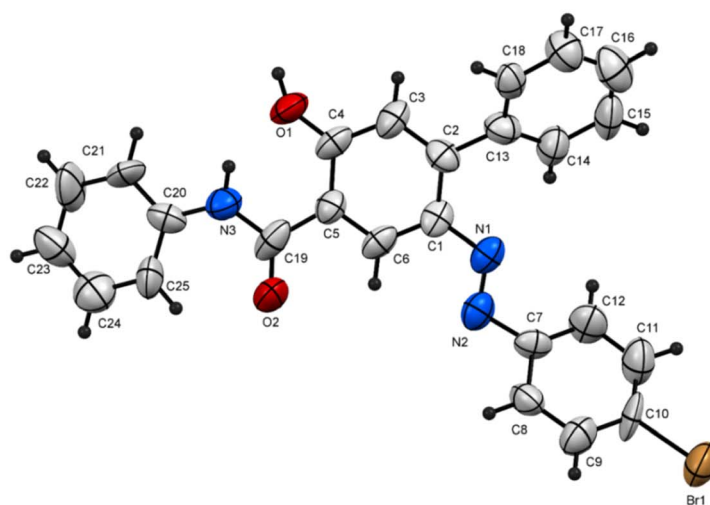
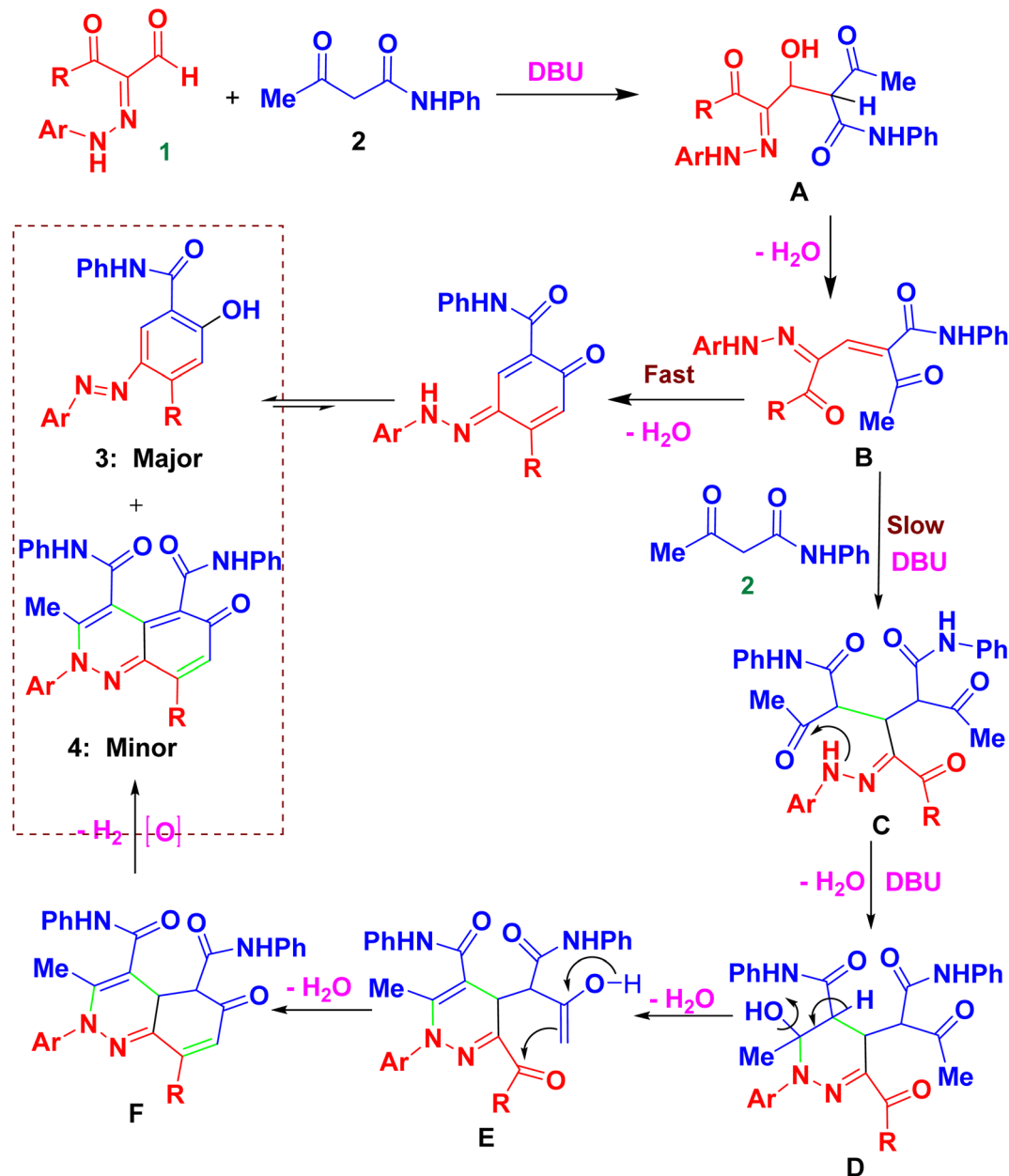
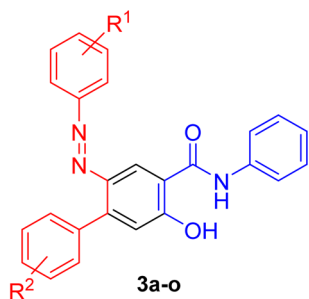
**3f****3h****3n**

Fig. 2 X-ray single crystals of compounds **3f**, **3h** and **3n** obtained from diffraction data.

this range, indicating that it has superior absorption properties in comparison to the other derivatives. The molar absorption coefficients for the azodyes **3a**, **3b**, **3i**, **3j**, **3f**, **3m**, and **3o** were calculated as 20 569, 30 036, 22 908, 25 639, 30 432, 12 852, and 240 212 $\text{M}^{-1} \text{cm}^{-1}$, respectively. The greater molar absorptivity (ϵ) obtained for the azodye **3o** (240 212 $\text{M}^{-1} \text{cm}^{-1}$) with

substituents $\text{R}^1 = 2\text{-NO}_2$ and $\text{R}^2 = \text{H}$ compared to the other azodyes, suggested that this particular chemical configuration possessed superior light absorption capabilities. The inclusion of the nitro group (NO_2) at the R^1 in the *ortho*-position was likely to introduce strong electron-withdrawing effects due to the inductive effect ($-I$), which resulted in a more effective



Scheme 4 A proposed mechanism for the chemoselective formation of **3** and **4**.Fig. 3 Molecular structures of the azodyes **3a–o** with various substituents (R^1 and R^2).

- | | |
|-----------------------------------|---------------------|
| 3a ; $R_1=4\text{-Br}$, | $R_2=4\text{-NO}_2$ |
| 3b ; $R_1=4\text{-Cl}$, | $R_2=4\text{-NO}_2$ |
| 3f ; $R_1=4\text{-Br}$, | $R_2=4\text{-Cl}$ |
| 3i ; $R_1=4\text{-Cl}$, | $R_2=4\text{-F}$ |
| 3j ; $R_1=4\text{-Br}$, | $R_2=4\text{-F}$ |
| 3m ; $R_1=4\text{-Cl}$, | $R_2=\text{H}$ |
| 3o ; $R_1=2\text{-NO}_2$, | $R_2=\text{H}$ |

interaction between the dye and the incident light. This increased number implies that the azodye **3o** had a better capacity to absorb photons and transform them into the excited states, making it more appropriate for the applications that require a strong light absorption, such as photovoltaic devices and light-harvesting systems.

In the emission spectra (Fig. 4b), compounds **3a**, **3f**, **3i**, **3j**, **3m**, and **3o** had comparable emission bands between 513–549 nm. This broad range showed that the emission properties of these compounds were comparable, with emission maxima between 520 and 540 nm. These emission bands were probably a result of similar photophysical processes that occurred within these substances. Notably, compound **3b**, which contains an electron-withdrawing NO_2 -group, exhibited a unique emission



Table 3 Photophysical properties of the synthesized azodye derivatives 3a–o

Azodyes	Absorption ^a , $\lambda_{\max/\text{abs}}$ (nm)	ϵ_{\max} ($\text{M}^{-1} \text{cm}^{-1}$)	Emission ^b , $\lambda_{\max/\text{em}}$ (nm)	Stokes shifts ^c (nm)
3a	475	20 569	551	76
3b	472	30 036	549	77
			709	237
3f	476	30 432	552	76
3i	475	22 908	549	74
3j	476	25 639	553	77
3m	444	12 852	513	69
3o	494	240 212	576	82

^a Determined in acetone at room temperature when the concentration of each compound is 1.0×10^{-5} M. ^b Excited at the longest wavelength of the absorption maxima. ^c Stokes shifts are provided as wavelength differences, $\Delta\lambda_{\max} = \lambda_{\max(\text{em})} - \lambda_{\max(\text{ex})}$.

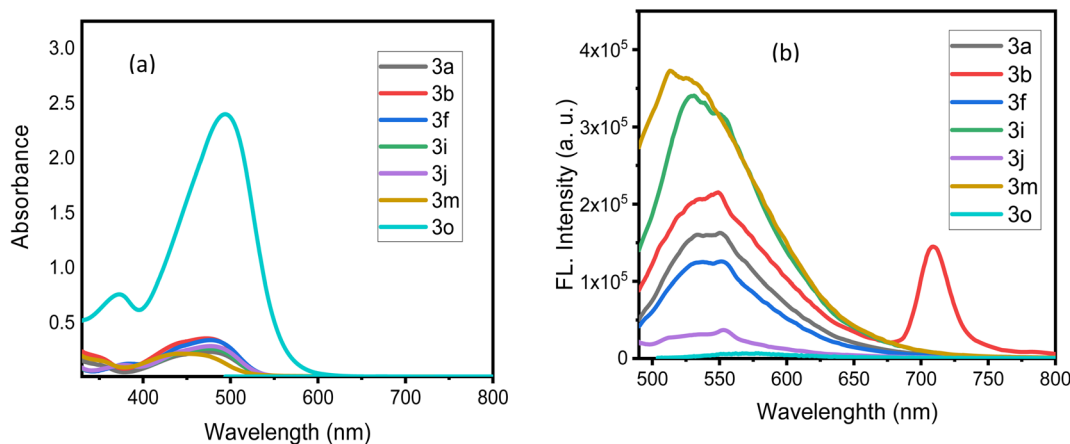


Fig. 4 (a) UV-Vis spectra of the azodye derivatives 3a–o; (b) emission spectra of the azodye derivatives 3a–o recorded in acetone.

behavior. It displayed a bathochromic (red) shift with an emission maximum at 709 nm, and a Stokes shift that was notably large at 237 nm (Table 3). The presence of the electron-withdrawing group, which greatly affected the electronic structure and energy levels of the molecule, was responsible for the dramatic red shift observed in compound 3b.

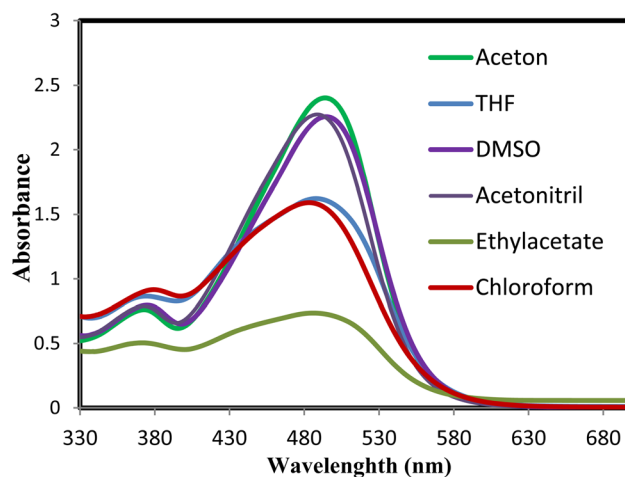
Overall, the presence of the electron-withdrawing NO_2 -group in compound 3b resulted in an extremely large Stokes shift due to a considerable red shift in the emission wavelength. These results demonstrated the significance of molecular structure and substitution patterns in modifying the photophysical characteristics of the azodyes.

Table 4 UV-Vis absorption and emission spectra of compound 3o in various polarity of solvents

Solvent	Absorption ^a , $\lambda_{\max/\text{abs}}$	ϵ_{\max} ($\text{M}^{-1} \text{cm}^{-1}$)	Emission ^b , ($\lambda_{\max/\text{em}}$)
DMSO	494	225 212	580
CH_3CN	489	227 258	574
Acetone	494	239 836	576
EtOAc	486	73 652	569
CHCl_3	483	157 062	567
THF	488	162 157	569

^a Concentration of 3o 1.0×10^{-5} M in different solvents. ^b Excitations were executed at or near the wavelength position of absorption maxima.

We examined the absorption and emission spectra of the azodye 3o in various organic solvents, such as acetone, dimethyl sulfoxide (DMSO), ethyl acetate (EtOAc), tetrahydrofuran (THF), acetonitrile (MeCN), and chloroform (CHCl_3). The results obtained are shown in Table 4 and Fig. 5 and 6. The broad band detected between 483 and 494 nm was due to an $n-\pi^*$ electronic

Fig. 5 Absorption and emission spectra of dye 3o in different organic solvents (acetone, DMSO, EtOAc, THF, MeCN, and CHCl_3).

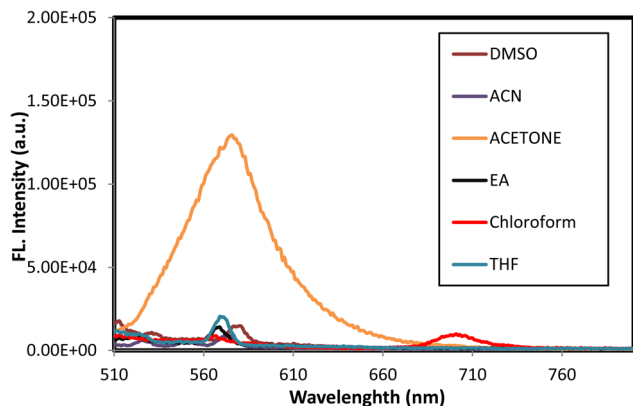


Fig. 6 Effect of solvent polarity on the emission spectra of the azodye **3o**. The emission maxima were shown for different solvents, including acetone, DMSO, EtOAc, THF, MeCN, and chloroform.

transition in the azoaromatic chromophore and intramolecular charge transfer. In addition, a shoulder in the region of 371–379 nm was noticed, which was indicative of the azobenzene molecule's easier π - π^* absorption.

Moreover, the effect of solvents on the azodye **3o** was examined. The 11 nm red shift in the absorption maxima when changing from DMSO to chloroform illustrated the influence of solvent polarity on the photophysical parameters. Variations in dipole moment in the excited state or changes in hydrogen bonding strength in polar liquids could account for this shift. The existence of hydrogen bonding could greatly influence numerous photophysical properties.⁸¹ Additionally, excited-state intermolecular proton transfer (ESIPT)⁸² might also influence the photophysical characteristics of the azodye **3o**. In contrast, the lower molar absorptivity values reported in other solvents such as chloroform ($157\,062\text{ M}^{-1}\text{ cm}^{-1}$), ethyl acetate ($73\,652\text{ M}^{-1}\text{ cm}^{-1}$), and THF ($162\,157\text{ M}^{-1}\text{ cm}^{-1}$) showed a relatively lower light absorption efficiency than acetone. These solvents might have weaker molecular connections or less suitable conditions for the absorption process of the azodye.

Regarding fluorescence characteristics, all the fluorescence maxima mentioned in Table 4 displayed a slight bathochromic shift as the solvent polarity increased, with the maximum emission wavelength in DMSO measured at 580 nm when stimulated at 494 nm. In the presence of DMSO, the extinction coefficient (ϵ) is approximately 1.4 times greater than that in the presence of chloroform, demonstrating that the polarity of the solvent influenced the intensity of emission. Higher intensities were recorded in polar solvents, as shown in Fig. 6.

The difference in molar absorptivity values between solvents implied that the choice of solvent could greatly affect the optical properties and absorption characteristics of the azodye **3o**. This information was useful for comprehending the solvatochromic effect and customizing the photophysical properties of the azodye for applications requiring precise control of light absorption and energy conversion processes.

These results illustrated the effect of solvent polarity on the photophysical properties of the azodye **3o** and scaled light on

the unique absorption and emission features of the synthesized azodye derivatives.

3. Experimental section

3.1. Materials and methods

All starting substrates were highly pure and purchased from Sigma-Aldrich. Griffin apparatus was used for measuring the melting points and were uncorrected. Thin layer chromatography (TLC) was established using Polygram SIL G/UV 254 TLC plates, and visualization was done under ultraviolet light at 254 and 365 nm. IR spectra were conducted using KBr disks in PerkinElmer System 2000 FTIR spectrophotometer. ^1H - and ^{13}C -NMR spectra were recorded at 600 and 150 MHz, respectively, on a Bruker DPX 400 or 600 super-conducting NMR spectrometer, at ambient temperature using DMSO- d_6 as a deuterated solvent and TMS as the internal standard (with chemical shifts given in parts per million (ppm)). Low-resolution electron impact mass spectrometry [MS (EI)] and high-resolution electron impact mass spectrometry [HRMS (EI)] were carried out using a high-resolution thermos spectrometer [GC-MS (DFS)] using a magnetic sector mass analyzer at 70.1 eV. Microwave (MW) experiments were conducted using a Discover LabMate CEM microwave instrument (300 W with CHEMDRIVER software; Matthews, NC). MW irradiation reactions were carried out in equipped closed pressured Pyrex tubes. The X-ray single-crystal data were performed involving a Bruker X8 Prospecter and a Rigaku RAXISRAPID diffractometer, and the single-crystal data collection was conducted using Cu K α radiation at ambient temperature. Solving and refining the structures was performed using the Bruker SHELXTL software package (refinement program-SHELXL97 and structure solution program-SHELXS-97). UV-Vis experiments were carried out on a Varian Cary 5 spectrometer from Agilent. Fluorescence assessments were conducted with Horiba Jobin Yvon-Fluoromax-4 equipped with a Time-Correlated Single Photon Counting (TCSPC) module.

3.2. Synthesis of the biphenyl-carboxamides **3a-o** and cinnoline derivatives **4a-o**

3.2.1. General method A. To a mixture of the appropriate arylhydrazonopropanal **1a-o** (0.5 mmol) and acetoacetanilide **2** (0.09 g, 0.5 mmol) in the appropriate solvent (MeOH, EtOH, *n*-hexane, toluene, chloroform, DMF or 1,4-dioxane) (6 mL), DBU (0.05 mL, 60 mol%) was added portion-wise. The mixture was heated at 40 °C for 2 h then left to cool to room temperature. The solvent was removed under reduced pressure and the residue was purified by preparative TLC (SiO₂ 60 mesh) using eluent (ethyl acetate : petroleum ether 40–60, 2 : 8 v/v).

3.2.2. General method B. To a mixture of the appropriate arylhydrazonopropanal **1a-o** (0.5 mmol) and acetoacetanilide **2** (0.09 g, 0.5 mmol) in the appropriate solvent (MeOH, EtOH, *n*-hexane, toluene, chloroform, DMF or 1,4-dioxane) (6 mL), DBU (0.05 mL, 60 mol%) was added portion-wise. The mixture was heated under microwave irradiating conditions at 40 °C and 200 W for the appropriate reaction time as listed in Table 2, then left to cool to room temperature. The solvent was removed



under reduced pressure and the residue was purified by preparative TLC (SiO₂ 60 mesh) using eluent (ethyl acetate : petroleum ether 40–60 °C, 2 : 8 v/v) to give the corresponding biphenyl-carboxamides **3a–o** and the cinnoline derivatives **4a–o**.

Notice: the cinnoline derivatives **4a–b** and **4e–m** were already characterized previously⁶⁸ and all data of the of currently prepared cinnolines **4a–b** and **4e–m** were in complete accordance with the reported ones. However, the newly synthesized herein, cinnoline derivatives **4c–d** and **4n–o** are fully characterized at the end of this part.

3.2.2.1. 2-(4-Bromophenylazo)-5-hydroxy-4'-nitro-N-phenyl-[1,1'-biphenyl]-4-carboxamide (3a). Orange solid, mp 266 °C; IR (KBr): ν/cm^{-1} 3247, 3080, 1635, 1578, 1474, 1385; ¹H NMR (DMSO-*d*₆): δ = 6.49 (s, 1H, Ar-H), 7.01 (t, *J* = 7.5 Hz, 1H, Ar-H), 7.31 (t, *J* = 7.8 Hz, 2H, Ar-H), 7.46 (d, *J* = 9 Hz, 2H, Ar-H), 7.60 (d, *J* = 8.4 Hz, 2H, Ar-H), 7.70 (d, *J* = 7.8 Hz, 2H, Ar-H), 7.78–7.71 (m, 2H, Ar-H), 8.28 (d, *J* = 8.4 Hz, 2H, Ar-H), 8.61 (s, 1H, Ar-H), 9.60 (b, 1H, NH), 14.43 (s, 1H, OH); ¹³C NMR (DMSO-*d*₆): δ = 118.47, 119.27, 119.50, 120.87, 122.31, 122.96, 123.37, 128.80, 131.35, 132.02, 134.88, 140.08, 146.28, 146.85, 165.21, 165.69 (Ar-C), 176.09 (CO). MS (EI): 518.10 [M]⁺. HRMS: calcd for C₂₅H₁₇BrN₄O₄: 517.04331, found 516.0428.

3.2.2.2. 2-(4-Chlorophenylazo)-5-hydroxy-4'-nitro-N-phenyl-[1,1'-biphenyl]-4-carboxamide (3b). Brown solid, mp 272–273 °C; IR (KBr): ν/cm^{-1} 3246, 3044, 2922, 1636, 1578, 1548, 1475, 1455, 1287; ¹H NMR (DMSO-*d*₆): δ = 6.54 (s, 1H, Ar-H), 7.01 (t, *J* = 7.2 Hz, 1H, Ar-H), 7.33 (t, *J* = 7.8 Hz, 2H, Ar-H), 7.34–7.31 (m, 2H, Ar-H), 7.56–7.54 (m, 2H, Ar-H), 7.73 (d, *J* = 7.8 Hz, 2H, Ar-H), 7.78 (d, *J* = 9 Hz, 2H, Ar-H), 8.28 (d, *J* = 9 Hz, 2H, Ar-H), 8.65 (s, 1H, Ar-H), 9.43 (b, 1H, NH), 14.45 (s, 1H, OH); ¹³C NMR (DMSO-*d*₆): δ = 118.45, 119.29, 119.49, 122.32, 122.46, 122.97, 123.06, 128.82, 129.12, 131.37, 132.25, 134.87, 140.10, 144.54, 146.29, 146.88, 151.89, 165.28, 165.71 (Ar-C), 176.04 (CO). MS (EI): 472.1 [M]⁺. HRMS: calcd for C₂₅H₁₇ClN₄O₄: 472.0938, found 472.0933.

3.2.2.3. 2-(3-Chlorophenylazo)-5-hydroxy-4'-nitro-N-phenyl-[1,1'-biphenyl]-4-carboxamide (3c). Orange solid, mp 235–236 °C; IR (KBr): ν/cm^{-1} 3249, 3047, 1637, 1578, 1475, 1388; ¹H NMR (DMSO-*d*₆): δ = 6.46 (s, 1H, Ar-H), 7.01 (t, *J* = 7.5 Hz, 1H, Ar-H), 7.80 (t, *J* = 7.2 Hz, 2H, Ar-H), 7.50–7.47 (m, 2H, Ar-H), 7.56–7.54 (m, 2H, Ar-H), 7.72–7.71 (m, 2H, Ar-H), 7.80–7.77 (m, 2H, Ar-H), 8.29–8.27 (m, 2H, Ar-H), 8.62 (s, 1H, Ar-H), 9.53 (br. s, 1H, NH), 14.46 (s, 1H, OH); ¹³C NMR (DMSO-*d*₆): δ = 118.44, 119.28, 119.46, 122.30, 122.45, 122.97, 123.06, 123.38, 128.38, 128.82, 129.12, 131.37, 132.20, 134.80, 140.10, 144.53, 146.28, 146.89, 151.89, 165.36, 165.71 (Ar-C), 176.10 (CO) MS (EI): 472.11 [M]⁺. HRMS: calcd for C₂₅H₁₇ClN₄O₄: 472.0938, found 472.0941.

3.2.2.4. 5-Hydroxy-2-(4-nitrophenylazo)-N-phenyl-[1,1'-biphenyl]-4-carboxamide (3d). Orange solid, mp 210–211 °C; IR (KBr): ν/cm^{-1} 3247, 3067, 1639, 1594, 1578, 1446, 1325; ¹H NMR (DMSO-*d*₆): δ = 6.50 (s, 1H, Ar-H), 7.02 (t, *J* = 10.8 Hz, 1H, Ar-H), 7.31–7.35 (m, 3H, Ar-H), 7.44 (t, *J* = 11.4 Hz, 2H, Ar-H), 7.57–7.55 (m, 2H, Ar-H), 7.73–7.71 (m, 2H, Ar-H), 7.81–7.79 (m, 2H, Ar-H), 8.30–8.28 (m, 2H, Ar-H), 8.61 (s, 1H, Ar-H), 9.59 (b, 1H, NH) 14.55 (s, 1H, OH); ¹³C NMR (DMSO-*d*₆): δ = 118.19, 119.27, 119.33, 121.58, 122.25, 122.42, 122.86, 128.21, 128.81, 129.06, 131.39, 134.83, 140.18, 144.31, 146.26, 147.04, 153.18, 165.35,

165.85 (Ar-C), 175.71 (CO). MS (EI): 438.18 [M]⁺. HRMS: calcd for C₂₅H₁₈N₄O₄: 438.1323, found 438.1323.

3.2.2.5. 4'-Chloro-5-hydroxy-N-phenyl-2-(phenylazo)-[1,1'-biphenyl]-4-carboxamide (3e). Orange solid, mp 253–254 °C; IR (KBr): ν/cm^{-1} 3266, 3090, 1640, 1585, 1476, 1389; ¹H NMR (DMSO-*d*₆): δ = 6.43 (s, 1H, Ar-H), 6.99 (t, *J* = 7.2 Hz, 1H, Ar-H), 7.32 (t, *J* = 7.8 Hz, 3H, Ar-H), 7.48–7.42 (m, 4H, Ar-H), 7.56–7.51 (m, 4H, Ar-H), 7.69 (d, *J* = 7.8 Hz, 2H, Ar-H), 8.56 (s, 1H, Ar-H), 9.51 (b, 1H, NH), 14.59 (s, 1H, OH); ¹³C NMR (DMSO-*d*₆): δ = 118.03, 118.70, 119.23, 121.50, 122.13, 122.62, 127.27, 128.02, 128.79, 129.03, 131.62, 131.95, 135.04, 138.60, 140.28, 145.21, 153.28, 165.36, 166.03 (Ar-C), 175.86 (CO). MS (EI): 427.10 [M]⁺. HRMS: calcd for C₂₅H₁₈ClN₃O₂: 427.1087, found 427.1083.

3.2.2.6. 2-(4-Bromophenylazo)-4'-chloro-5-hydroxy-N-phenyl-[1,1'-biphenyl]-4-carboxamide (3f). Orange solid, mp 253–254 °C; IR (KBr): ν/cm^{-1} 3252, 3050, 2945, 1638, 1590, 1579, 1453, 1386; ¹H NMR (DMSO-*d*₆): δ = 6.44 (s, 1H, Ar-H), 6.99 (t, *J* = 7.8 Hz, 1H, Ar-H), 7.32 (t, *J* = 7.8 Hz, 2H, Ar-H), 7.51–7.50 (m, 4H, Ar-H), 7.53–7.52 (m, 2H, Ar-H), 7.63–7.61 (m, 2H, Ar-H), 7.31 (d, *J* = 7.8 Hz, 2H, Ar-H), 8.59 (s, 1H, Ar-H), 9.54 (b, 1H, OH) 14.48 (s, 1H, NH); ¹³C NMR (DMSO-*d*₆): δ = 118.32, 118.89, 119.24, 120.66, 122.21, 123.29, 127.31, 128.79, 131.71, 131.92, 132.01, 135.10, 138.43, 140.18, 145.45, 152.30, 165.22, 165.86 (Ar-C), 176.24 (CO). MS (EI): 507.1 [M]⁺. HRMS: calcd for C₂₅H₁₇BrClN₃O₂: 505.01926, found 505.01933. Single crystals of **3f** were obtained by the slow evaporation of a CHCl₃/CH₃OH solution of **3f**. Crystal data: C₂₅H₁₇BrClN₃O₂, triclinic, *a* = 8.4153 Å, *b* = 12.6081 Å, *c* = 14.8911 Å, α = 92.688°, β = 97.266°, γ = 94.691°, *V* = 1559.4 Å³, *T* = 293 K, space group: *P* $\bar{1}$, *Z* = 2, calculated density = 1.403 g cm⁻³, no. of reflection measured 5471, θ_{max} = 24.987, *R*₁ = 0.0597.⁸⁰

3.2.2.7. 4'-Bromo-2-(4-chlorophenylazo)-5-hydroxy-N-phenyl-[1,1'-biphenyl]-4-carboxamide (3g). Yellow solid, mp 221–223 °C; IR (KBr): ν/cm^{-1} 3252, 3050, 1637, 1577, 1483, 1387; ¹H NMR (DMSO-*d*₆): δ = 6.42 (s, 1H, Ar-H), 6.99 (t, *J* = 7.2 Hz, 1H, Ar-H), 7.31 (t, *J* = 7.8 Hz, 2H, Ar-H), 7.44 (dd, *J* = 2.1, 6.3 Hz, 2H, Ar-H), 7.48 (dd, *J* = 1.8, 6.6 Hz, 2H, Ar-H), 7.53 (dd, *J* = 1.8, 6.6 Hz, 2H, Ar-H), 7.58 (dd, *J* = 1.8, 6.6 Hz, 2H, Ar-H), 7.69 (d, *J* = 7.8 Hz, 2H, Ar-H), 8.57 (s, 1H, Ar-H), 9.45 (s, 1H, OH), 14.49 (s, 1H, OH); ¹³C NMR (DMSO-*d*₆): δ = 118.33, 118.89, 119.28, 120.38, 122.26, 122.71, 126.83, 128.83, 129.13, 130.26, 132.31, 135.07, 138.84, 140.23, 145.64, 151.99, 165.37, 165.89 (Ar-C), 176.18 (CO). MS (EI): 507.10 [M]⁺; HRMS: calcd for C₂₅H₁₇BrClN₃O₂: 505.01926, found 505.0265.

3.2.2.8. 4'-Bromo-2-(4-bromophenylazo)-5-hydroxy-N-phenyl-[1,1'-biphenyl]-4-carboxamide (3h). Yellow solid, mp 159–160 °C; IR (KBr): ν/cm^{-1} 3250, 3055, 2970, 1660, 1590, 1562, 1475, 1295; ¹H NMR (DMSO-*d*₆): δ = 6.42 (s, 1H, Ar-H), 6.99 (t, *J* = 6.6 Hz, 2H, Ar-H), 7.31 (t, *J* = 7.8 Hz, 2H, Ar-H), 7.48–7.44 (m, 4H, Ar-H), 7.72–7.68 (m, 5H, Ar-H), 8.57 (s, 1H, Ar-H), 9.53 (s, 1H, NH), 14.47 (s, 1H, OH); ¹³C NMR (DMSO-*d*₆): δ = 118.20, 118.70, 119.29, 120.50, 122.14, 122.84, 123.27, 126.84, 127.37, 128.89, 130.19, 131.86, 135.19, 139.64, 140.33, 146.97, 152.38, 164.66, 165.98 (Ar-C), 176.43 (CO). MS (EI): 551.10 [M]⁺. HRMS: calcd for C₂₅H₁₇Br₂N₃O₂: 548.9687, found 548.9681. Single crystals of **3h** were obtained by the slow evaporation of a CHCl₃/CH₃OH solution of **3h**. Crystal data: C₂₅H₁₇Br₂N₃O₂, monoclinic, *a* =



11.5200 Å, $b = 12.9090$ Å, $c = 21.274$ Å, $\alpha = 90^\circ$, $\beta = 93.818^\circ$, $\gamma = 90^\circ$, $V = 315.7$ Å³, $T = 150$ K, space group: $P2_1/c_1$, $Z = 4$, calculated density = 1.480 g cm⁻³, no. of reflection measured 5947, $\theta_{\max} = 25.630$, $R_1 = 0.0672$.⁸⁰

3.2.2.9. *2-(4-Chlorophenylazo)-4'-fluoro-5-hydroxy-N-phenyl-[1,1'-biphenyl]-4-carboxamide (3i)*. Orange solid, mp 269–270 °C; IR (KBr): ν/cm^{-1} 3436, 3266, 2936, 1637, 1597, 1578, 1419, 1390; ¹H NMR (DMSO-*d*₆): $\delta = 6.43$ (s, 1H, Ar-H), 7.00 (t, $J = 7.5$ Hz, 1H, Ar-H), 7.25–7.22 (m, 2H, Ar-H), 7.32 (t, $J = 7.8$ Hz, 2H, Ar-H), 7.54–7.46 (m, 6H, Ar-H), 7.70 (d, $J = 8.4$ Hz, 2H, Ar-H), 8.57 (s, 1H, Ar-H), 9.50 (b, 1H, NH), 14.49 (s, 1H, OH); ¹³C NMR (DMSO-*d*₆): $\delta = 114.04$, 114.18, 118.24, 118.72, 119.25, 122.20, 122.76, 122.97, 128.81, 129.08, 131.99, 132.04, 135.22, 135.88, 135.90, 140.22, 145.74, 152.03, 160.64, 162.26, 165.36, 165.94 (Ar-C), 176.21 (CO). MS (EI): 445.20 [M]⁺. HRMS: calcd for C₂₅H₁₇ClFN₃O₂: 445.09933, found 445.0988.

3.2.2.10. *2-(4-Bromophenylazo)-4'-fluoro-5-hydroxy-N-phenyl-[1,1'-biphenyl]-4-carboxamide (3j)*. Orange solid, mp 257–258 °C; IR (KBr): ν/cm^{-1} 3253, 2935, 1637, 1595, 1548, 1417, 1385; ¹H NMR (DMSO-*d*₆): $\delta = 6.42$ (s, 1H, Ar-H), 7.00 (t, $J = 7.2$ Hz, 1H, Ar-H), 7.23 (t, $J = 7.8$ Hz, 2H, Ar-H), 7.29–7.32 (m, 2H, Ar-H), 7.46 (d, $J = 8.64$ Hz, 2H, Ar-H), 7.50–7.52 (m, 2H, Ar-H), 7.60 (d, $J = 8.64$ Hz, 2H, Ar-H), 7.69 (d, $J = 7.56$ Hz, 2H, Ar-H), 8.57 (s, 1H, Ar-H), 9.50 (b, 1H, NH), 14.49 (s, 1H, OH); ¹³C NMR (DMSO-*d*₆): $\delta = 114.12$, 114.26, 118.30, 118.81, 119.35, 120.77, 122.34, 122.84, 123.38, 128.88, 132.07, 132.11, 135.42, 135.89, 140.81, 152.81, 152.36, 160.72, 162.34, 165.96, (Ar-C), 176.16 (CO). MS (EI): 491.0 [M + 2]⁺. HRMS: calcd for C₂₅H₁₇BrFN₃O₂: 489.0488, found 489.0483.

3.2.2.11. *2-(4-Bromophenylazo)-5-hydroxy-4'-methoxy-N-phenyl-[1,1'-biphenyl]-4-carboxamide (3k)*. Orange solid, mp 255–257 °C; IR (KBr): ν/cm^{-1} ; 3270, 3053, 1657, 1543, 1474, 1391; ¹H NMR (DMSO-*d*₆): $\delta = 3.85$ (s, 3H, OCH₃), 6.54 (s, 1H, Ar-H), 6.97 (t, $J = 7.8$ Hz, 1H, Ar-H), 7.14–7.00 (m, 4H, Ar-H), 7.26–7.19 (m, 4H, Ar-H), 7.49–7.30 (m, 1H, Ar-H), 7.83–7.69 (m, 1H, Ar-H), 8.27 (d, $J = 9$ Hz, 2H, Ar-H), 8.55 (s, 1H, Ar-H), 9.75 (b, 1H, NH), 14.50 (s, 1H, OH); ¹³C NMR (DMSO-*d*₆): $\delta = 55.69$ (OCH₃), 114.00, 115.73, 119.99, 120.28, 123.56, 127.80, 128.61, 128.68, 128.89, 132.00, 133.26, 134.90, 139.28, 139.97, 141.90, 142.29, 143.43, 152.36, 160.21 (Ar-C), 179.45 (CO). MS (EI): 500.1 [M]⁺. HRMS: calcd for C₂₆H₂₀BrN₃O₃: 501.0688, found 501.0674.

3.2.2.12. *5-Hydroxy-4'-methoxy-2-(2-nitrophenylazo)-N-phenyl-[1,1'-biphenyl]-4-carboxamide (3l)*. Orange solid, mp 235–237 °C; IR (KBr): ν/cm^{-1} 3270, 3069, 2924, 1685, 1601, 1542, 1473, 1309; ¹H NMR (DMSO-*d*₆): $\delta = 3.82$ (s, 3H, OCH₃), 7.06 (dd, $J = 1.8, 6.6$ Hz, 2H, Ar-H), 7.39–7.37 (m, 2H, Ar-H), 7.45 (d, $J = 8.4$ Hz, 3H, Ar-H), 7.70–7.67 (m, 1H, Ar-H), 7.73 (d, $J = 7.8$ Hz, 2H, Ar-H) 7.81–7.78 (m, 2H, Ar-H), 8.05 (dd, $J = 1.2, 8.4$ Hz, 2H, Ar-H), 8.19 (s, 1H, Ar-H), 9.57 (b, 1H, NH), 14.50 (s, 1H, OH); ¹³C NMR (DMSO-*d*₆): $\delta = 55.18$, 113.53, 118.06, 118.11, 118.72, 119.68, 120.36, 124.00, 124.11, 128.76, 129.24, 130.68, 131.66, 133.58, 138.34, 141.79, 144.73, 146.19, 146.77, 159.42, 164.34 (Ar-C), 176.42 (CO). MS (EI): 468.1 [M]⁺. HRMS: calcd for C₂₆H₂₀N₄O₅: 468.1433, found 468.1428.

3.2.2.13. *2-(4-Chlorophenylazo)-5-hydroxy-N-phenyl-[1,1'-biphenyl]-4-carboxamide (3m)*. Gray yellow solid, mp 156–158 °C; IR (KBr): ν/cm^{-1} 3252, 3050, 2928, 1638, 1598, 1582, 1434, 1389;

¹H NMR (DMSO-*d*₆): $\delta = 6.46$ (s, 1H, Ar-H), 7.00 (t, $J = 7.5$ Hz, 1H, Ar-H), 7.25 (t, $J = 7.2$ Hz, 2H, Ar-H), 7.38–7.35 (m, 1H, Ar-H), 7.42 (t, $J = 7.5$ Hz, 2H, Ar-H), 7.50–7.46 (m, 4H, Ar-H), 7.56–7.54 (m, 2H, Ar-H), 7.72 (d, $J = 8.4$ Hz, 2H, Ar-H), 8.58 (s, 1H, Ar-H), 9.60 (s, 1H, NH), 14.50 (s, 1H, OH); ¹³C NMR (DMSO-*d*₆): $\delta = 118.15$, 118.59, 119.24, 122.17, 122.76, 122.95, 126.85, 127.28, 128.79, 129.03, 130.19, 131.94, 140.23, 146.84, 152.04, 165.36, 165.97 (Ar-C), 176.01 (CO). MS (EI): 427.25 [M]⁺. HRMS: calcd for C₂₅H₁₈ClN₃O₂: 427.1087, found 427.1082.

3.2.2.14. *2-(4-Bromophenylazo)-5-hydroxy-N-phenyl-[1,1'-biphenyl]-4-carboxamide (3n)*. Orange solid, mp 252–253 °C; IR (KBr): ν/cm^{-1} 3250, 3048, 2932, 1639, 1582, 1569, 1473, 1432, 1299; ¹H NMR (DMSO-*d*₆): $\delta = 6.43$ (s, 1H, Ar-H), 7.00 (t, $J = 7.2$ Hz, 1H, Ar-H), 7.36–7.30 (m, 3H, Ar-H), 7.41 (t, $J = 6.6$ Hz, 2H, Ar-H), 7.48–7.45 (m, 4H, Ar-H), 7.60–7.58 (m, 2H, Ar-H), 7.69 (d, $J = 7.2$ Hz, 2H, Ar-H), 8.57 (s, 1H, Ar-H), 9.70 (b, 1H, NH), 14.53 (s, 1H, OH); ¹³C NMR (DMSO-*d*₆): $\delta = 118.19$, 118.60, 119.23, 120.50, 122.14, 122.84, 123.27, 126.84, 127.27, 128.79, 130.19, 131.94, 135.29, 139.64, 140.26, 146.87, 152.38, 164.66, 165.98 (Ar-C), 176.31 (CO). MS (EI): 472.10 [M]⁺. HRMS: calcd for C₂₅H₁₈BrN₃O₂: 471.05823, found 471.0577. Single crystals of **3n** were obtained by the slow evaporation of a CHCl₃/CH₃OH solution of **3n**. Crystal data: C₂₅H₁₈BrN₃O₂, monoclinic, $a = 12.653$ Å, $b = 8.433$ Å, $c = 28.374$ Å, $\alpha = 90^\circ$, $\beta = 96.333^\circ$, $\gamma = 90^\circ$, $V = 3009.2$ Å³, $T = 293$ K, space group: $P2_1/c_1$, $Z = 4$, calculated density = 1.379 g cm⁻³, no. of reflection measured 5304, $\theta_{\max} = 25.036$, $R_1 = 0.0830$.⁸⁰

3.2.2.15. *5-Hydroxy-2-(2-nitrophenylazo)-N-phenyl-[1,1'-biphenyl]-4-carboxamide (3o)*. Orange solid, mp 213–214 °C; IR (KBr): ν/cm^{-1} 3270, 3053, 2922, 1657, 1543, 1474, 1474, 1391; ¹H NMR (DMSO-*d*₆): $\delta = 6.47$ (s, 1H, Ar-H), 7.03 (t, $J = 7.5$ Hz, 1H, Ar-H), 7.43–7.32 (m, 7H, Ar-H), 7.51–7.49 (m, 2H, Ar-H), 7.60 (t, $J = 6.9$ Hz, 1H, Ar-H), 7.73–7.72 (m, 2H, Ar-H), 7.87 (d, $J = 7.8$ Hz, 1H, Ar-H), 8.55 (s, 1H, Ar-H), 14.28 (s, 1H, OH); ¹³C NMR (DMSO-*d*₆): $\delta = 118.17$, 119.04, 119.18, 119.26, 122.35, 123.04, 123.44, 126.99, 127.37, 127.45, 128.81, 130.09, 132.48, 136.10, 139.34, 140.04, 145.47, 146.77, 147.82, 164.99, 165.56 (Ar-C), 177.31 (CO). MS (EI): 437.13 [M]⁺. HRMS: calcd for C₂₅H₁₈N₄O₄: 438.13280, found 438.1323.

3.2.2.16. *2-(4-Bromophenyl)-3-methyl-8-(4-nitrophenyl)-6-oxo-N⁴,N⁵-diphenyl-2,6-dihydrocinnoline-4,5-dicarboxamide (4a)*. Orange solid, Lit.⁶⁸ mp 302–304 °C; ¹H NMR (DMSO-*d*₆): $\delta = 2.36$ (s, 3H, CH₃), 6.96–7.26 (m, 7H, Ar-H), 7.47 (d, $J = 7.2$ Hz, 2H, Ar-H), 7.56 (d, $J = 7.8$ Hz, 2H, Ar-H), 7.60–7.65 (m, 2H, Ar-H), 7.86–7.95 (m, 4H, Ar-H), 8.27 (d, $J = 7.8$ Hz, 1H, Ar-H), 8.34 (d, $J = 7.8$ Hz, 1H, Ar-H), 10.45 (s, 1H, NH), 10.57 (s, 1H, NH); ¹³C NMR (DMSO-*d*₆): $\delta = 19.39$ (CH₃), 115.70, 115.81, 119.52, 119.82, 121.76, 122.60, 122.98, 123.16, 123.21, 123.60, 124.03, 124.69, 127.20, 128.12, 128.40, 130.78, 131.08, 131.48, 132.81, 135.92, 136.85, 138.74, 139.44, 140.35, 140.45, 141.66, 142.28, 143.46, 147.41 (Ar-C), 162.28, 164.18, 178.68 (C=O).

3.2.2.17. *2-(4-Chlorophenyl)-3-methyl-8-(4-nitrophenyl)-6-oxo-N⁴,N⁵-diphenyl-2,6-dihydrocinnoline-4,5-dicarboxamide (4b)*. Orange crystals, Lit.⁶⁸ mp 249–251 °C; ¹H NMR (DMSO-*d*₆): $\delta = 2.35$ (s, 3H, CH₃), 6.95 (t, $J = 7.5$ Hz, 1H, Ar-H), 7.07 (t, $J = 7.5$ Hz, 1H, Ar-H), 7.12 (t, $J = 7.5$ Hz, 2H, Ar-H), 7.22–7.25 (m, 3H, Ar-H), 7.47 (d, $J = 7.8$ Hz, 2H, Ar-H), 7.55 (d, $J = 7.8$ Hz, 2H, Ar-H), 7.68–



7.72 (m, 4H, Ar-H), 7.94 (d, $J = 8.4$ Hz, 2H, Ar-H), 8.26 (d, $J = 8.4$ Hz, 2H, Ar-H), 10.41 (s, 1H, NH), 10.56 (s, 1H, NH); ^{13}C NMR (DMSO- d_6): $\delta = 19.87$ (CH₃), 116.44, 119.99, 120.30, 123.09, 123.47, 124.09, 124.59, 127.61, 128.40, 128.61, 128.89, 130.37, 131.98, 135.07, 136.70, 139.18, 139.92, 140.66, 141.72, 142.35, 142.64, 147.86 (Ar-C), 162.92, 164.55, 178.84 (C=O).

3.2.2.18. *2-(3-Chlorophenyl)-3-methyl-8-(4-nitrophenyl)-6-oxo- N^4,N^5 -diphenyl-2,6-dihydrocinnoline-4,5-dicarboxamide* (**4c**). Orange crystals, mp 281.283 °C; IR (KBr): ν/cm^{-1} 3246 (NH), 1675 (C=O), 1601 (C=C); ^1H NMR (DMSO- d_6): $\delta = 2.36$ (s, 3H, CH₃), 6.96 (t, $J = 7.32$ Hz, 1H, Ar-H), 7.01–7.02 (m, 2H, Ar-H), 7.07–7.09 (m, 2H, Ar-H), 7.55–7.59 (m, 2H, Ar-H), 7.13 (t, $J = 7.86$ Hz, 2H, Ar-H), 7.25 (t, $J = 7.89$ Hz, 2H, Ar-H), 7.47 (d, $J = 7.56$ Hz, 2H, Ar-H), 7.55 (d, $J = 7.56$ Hz, 2H, Ar-H), 7.60–7.64 (m, 6H, Ar-H), 7.87 (d, $J = 8.76$ Hz, 2H, Ar-H), 10.50 (s, 1H, NH), 10.55 (s, 1H, NH); ^{13}C NMR (DMSO- d_6): $\delta = 19.36$ (CH₃), 113.51, 115.22, 119.50, 119.80, 122.54, 123.06, 123.52, 123.91, 127.31, 128.13, 128.40, 131.50, 132.77, 134.40, 138.78, 139.47, 140.69, 142.95, 159.71 (Ar-C) 162.29, 164.28, 178.96 (C=O). MS (EI): 629.1 [M – 1]⁺. HRMS: calcd for C₃₅H₂₄ClN₅O₅: 629.1465, found 629.1423.

3.2.2.19. *3-Methyl-2-(4-nitrophenyl)-6-oxo- N^4,N^5 ,8-triphenyl-2,6-dihydrocinnoline-4,5-dicarboxamide* (**4d**). Yellow crystals, mp 246–247 °C; IR (KBr): ν/cm^{-1} 3251 (NH), 1668 (C=O), 1599 (C=C); ^1H NMR (DMSO- d_6): $\delta = 2.36$ (s, 3H, CH₃), 6.96 (t, $J = 7.35$ Hz, 1H, Ar-H), 7.07–7.14 (m, 3H, Ar-H), 7.22–7.26 (m, 3H, Ar-H), 7.47–7.48 (m, 2H, Ar-H), 7.55–7.59 (m, 3H, Ar-H), 7.63–7.66 (m, 4H, Ar-H), 7.94–7.95 (m, 2H, Ar-H), 8.27–8.29 (m, 2H, Ar-H), 10.45 (s, 1H, NH), 10.60 (s, 1H, NH); ^{13}C NMR (DMSO- d_6): $\delta = 19.41$ (CH₃), 115.66, 119.51, 119.82, 122.59, 122.97, 123.58, 124.28, 125.97, 127.23, 128.13, 128.40, 129.85, 130.00, 131.50, 136.25, 138.73, 139.45, 140.08, 141.95, 142.26, 142.52, 147.36 (Ar-C) 162.51, 164.14, 178.25 (C=O). MS (EI): 592.85 [M – 2]⁺. HRMS: calcd for C₃₅H₂₅N₅O₅: 595.1855, found 595.1857.

3.2.2.20. *8-(4-Chlorophenyl)-3-methyl-6-oxo- N^4,N^5 ,2-triphenyl-2,6-dihydrocinnoline-4,5-dicarboxamide* (**4e**). Orange crystals, Lit.⁶⁸ mp 268–270 °C; ^1H NMR (DMSO- d_6): $\delta = 2.35$ (s, 3H, CH₃), 6.95 (t, $J = 6.9$ Hz, 1H, Ar-H), 7.06 (t, $J = 6.6$ Hz, 1H, Ar-H), 7.11 (m, 3H, Ar-H), 7.24 (t, $J = 7.8$ Hz, 2H, Ar-H), 7.46–7.47 (m, 2H, Ar-H), 7.49–7.50 (m, 2H, Ar-H), 7.55–7.62 (m, 3H, Ar-H), 7.64 (d, $J = 4.2$ Hz, 4H, Ar-H), 7.66–7.68 (m, 2H, Ar-H), 10.48 (s, 1H, NH), 10.55 (s, 1H, NH); ^{13}C NMR (DMSO- d_6): $\delta = 19.35$ (CH₃), 115.17, 119.48, 119.79, 123.50, 124.20, 125.94, 127.33, 127.97, 128.09, 128.36, 129.78, 131.90, 133.46, 134.43, 135.41, 138.74, 139.43, 141.73, 142.56 (Ar-C) 162.59, 164.20, 178.96 (C=O).

3.2.2.21. *2-(4-Bromophenyl)-8-(4-chlorophenyl)-3-methyl-6-oxo- N^4,N^5 -diphenyl-2,6-dihydrocinnoline-4,5-dicarboxamide* (**4f**). Pale yellow crystals, Lit.⁶⁸ mp 274–276 °C; ^1H NMR (DMSO- d_6): $\delta = 2.35$ (s, 3H, CH₃); 6.95 (t, $J = 7.25$ Hz, 1H, Ar-H), 7.06 (t, $J = 7.2$ Hz, 1H, Ar-H), 7.10–7.13 (m, 3H, Ar-H), 7.24 (t, $J = 7.8$ Hz, 2H, Ar-H), 7.45 (d, $J = 7.2$ Hz, 2H, Ar-H), 7.50 (d, $J = 8.4$ Hz, 2H, Ar-H), 7.53 (d, $J = 7.8$ Hz, 2H, Ar-H), 7.61 (d, $J = 8.4$ Hz, 2H, Ar-H), 7.67 (d, $J = 8.4$ Hz, 2H, Ar-H), 7.85 (d, $J = 8.4$ Hz, 2H, Ar-H), 10.44 (s, 1H, NH), 10.55 (s, 1H, NH); ^{13}C NMR (DMSO- d_6): $\delta = 19.39$ (CH₃), 115.56, 119.52, 119.82, 122.59, 123.56, 123.16, 123.58, 124.04, 127.22, 128.03, 128.13, 128.15, 128.41, 131.94,

132.80, 133.55, 134.36, 135.39, 138.74, 139.45, 140.40, 141.63, 141.73, 142.03 (Ar-C), 162.55, 164.18, 178.68 (C=O).

3.2.2.22. *8-(4-Bromophenyl)-2-(4-chlorophenyl)-3-methyl-6-oxo- N^4,N^5 -diphenyl-2,6-dihydrocinnoline-4,5-dicarboxamide* (**4g**). Orange crystals, Lit.⁶⁸ mp 276–278 °C; ^1H NMR (DMSO- d_6): $\delta = 2.34$ (s, 3H, CH₃), 6.95 (t, $J = 7.2$ Hz, 1H, Ar-H), 7.06 (t, $J = 7.2$ Hz, 1H, Ar-H), 7.11 (m, 3H, Ar-H), 7.24 (t, $J = 8.1$ Hz, 2H, Ar-H), 7.46 (d, $J = 7.8$ Hz, 2H, Ar-H), 7.54 (d, $J = 7.8$ Hz, 2H, Ar-H), 7.60–7.65 (m, 4H, Ar-H), 7.67–7.73 (m, 4H, Ar-H), 10.44 (s, 1H, NH), 10.54 (s, 1H, NH); ^{13}C NMR (DMSO- d_6): $\delta = 19.37$ (CH₃), 115.54, 119.49, 119.79, 122.24, 122.56, 123.55, 124.00, 127.22, 128.11, 129.85, 130.94, 132.21, 134.55, 134.73, 135.36, 138.73, 139.44, 140.31, 141.29, 141.67, 142.07 (Ar-C), 162.53, 164.15, 179.43 (C=O).

3.2.2.23. *2,8-Di(4-bromophenyl)-3-methyl-6-oxo- N^4,N^5 -diphenyl-2,6-dihydrocinnoline-4,5-dicarboxamide* (**4h**). Pale yellow solid, Lit.⁶⁸ mp 268–270 °C; ^1H NMR (DMSO- d_6): $\delta = 2.34$ (s, 3H, CH₃), 6.95 (t, $J = 7.5$ Hz, 1H, Ar-H), 7.06 (t, $J = 7.5$ Hz, 1H, Ar-H), 7.10–7.13 (m, 3H, Ar-H), 7.24 (t, $J = 7.8$ Hz, 2H, Ar-H), 7.46 (d, $J = 7.8$ Hz, 2H, Ar-H), 7.54 (d, $J = 7.8$ Hz, 2H, Ar-H), 7.59–7.65 (m, 6H, Ar-H), 7.86 (d, $J = 9$ Hz, 2H, Ar-H), 10.44 (s, 1H, NH), 10.54 (s, 1H, NH); ^{13}C NMR (DMSO- d_6): $\delta = 19.37$ (CH₃), 115.55, 119.49, 119.79, 122.24, 122.56, 123.15, 123.55, 124.01, 127.20, 128.11, 128.14, 128.39, 130.94, 132.20, 132.79, 134.72, 135.35, 138.72, 139.44, 140.31, 141.60, 141.71, 142.05 (Ar-C), 162.52, 164.15, 178.65 (C=O).

3.2.2.24. *2-(4-Chlorophenyl)-8-(4-fluorophenyl)-3-methyl-6-oxo- N^4,N^5 -diphenyl-2,6-dihydrocinnoline-4,5-dicarboxamide* (**4i**). Yellow solid, Lit.⁶⁸ mp 271–273 °C; ^1H NMR (DMSO- d_6): $\delta = 2.35$ (s, 3H, CH₃), 6.95 (t, $J = 7.5$ Hz, 1H, Ar-H), 7.06 (t, $J = 7.2$ Hz, 1H, Ar-H), 7.09 (s, 1H, Ar-H), 7.12 (t, $J = 7.8$ Hz, 2H, Ar-H), 7.22–7.29 (m, 4H, Ar-H), 7.45 (d, $J = 7.2$ Hz, 2H, Ar-H), 7.55 (d, $J = 7.2$ Hz, 2H, Ar-H), 7.67–7.72 (m, 6H, Ar-H), 10.46 (s, 1H, NH), 10.55 (s, 1H, NH); ^{13}C NMR (DMSO- d_6): $\delta = 19.38$ (CH₃), 114.86, 115.00, 115.44, 119.51, 119.80, 122.57, 123.56, 124.01, 127.25, 127.92, 128.12, 128.41, 129.83, 131.87, 131.89, 132.26, 132.31, 134.51, 135.26, 138.75, 139.46, 140.54, 141.33, 141.61, 142.20 (Ar-C), 162.59, 164.20, 178.75 (C=O).

3.2.2.25. *2-(4-Bromophenyl)-8-(4-fluorophenyl)-3-methyl-6-oxo- N^4,N^5 -diphenyl-2,6-dihydrocinnoline-4,5-dicarboxamide* (**4j**). Yellow crystals, Lit.⁶⁸ mp 267–269 °C; ^1H NMR (DMSO- d_6): $\delta = 2.35$ (s, 3H, CH₃); 6.95 (t, $J = 7.2$ Hz, 1H, Ar-H), 7.06 (t, $J = 7.5$ Hz, 1H, Ar-H), 7.09 (s, 1H, Ar-H), 7.12 (t, $J = 7.8$ Hz, 2H, Ar-H), 7.22–7.29 (m, 4H, Ar-H), 7.47 (d, $J = 7.2$ Hz, 2H, Ar-H), 7.55 (d, $J = 7.2$ Hz, 2H, Ar-H), 7.61 (d, $J = 8.4$ Hz, 2H, Ar-H), 7.68–7.71 (m, 2H, Ar-H), 7.85 (d, $J = 9$ Hz, 2H, Ar-H), 10.46 (s, 1H, NH), 10.57 (s, 1H, NH); ^{13}C NMR (DMSO- d_6): $\delta = 19.38$ (CH₃), 114.85, 114.99, 115.45, 119.50, 122.55, 123.10, 123.53, 124.02, 127.24, 128.11, 128.14, 128.39, 131.87, 132.24, 132.29, 132.76, 135.25, 138.75, 139.45, 140.54, 141.54, 141.74, 142.19, 161.54, 162.27 (Ar-C) 163.17, 164.19, 178.75 (C=O).

3.2.2.26. *8-(4-Anisyl)-2-(4-bromophenyl)-3-methyl-6-oxo- N^4,N^5 -diphenyl-2,6-dihydrocinnoline-4,5-dicarboxamide* (**4k**). Orange crystals, Lit.⁶⁸ mp 252–254 °C; ^1H NMR (DMSO- d_6): $\delta = 2.34$ (s, 3H, CH₃), 3.79 (s, 3H, OCH₃), 6.97 (t, $J = 7.5$ Hz, 1H, Ar-H), 7.02 (d, $J = 8.4$ Hz, 2H, Ar-H), 7.07 (t, $J = 7.5$ Hz, 2H, Ar-H), 7.12 (t, $J = 7.8$ Hz, 2H, Ar-H), 7.24 (t, $J = 7.8$ Hz, 2H, Ar-H), 7.46



(d, $J = 7.8$ Hz, 2H, Ar-H), 7.55–7.62 (m, 6H, Ar-H), 7.86 (d, $J = 8.4$ Hz, 2H, Ar-H), 10.49 (s, 1H, NH), 10.54 (s, 1H, NH); ^{13}C NMR (DMSO- d_6): $\delta = 19.39$ (CH_3), 55.20 (OCH_3), 113.52, 115.24, 119.51, 119.80, 122.56, 123.08, 123.54, 123.92, 127.32, 127.74, 128.14, 128.19, 128.42, 131.52, 132.78, 134.41, 138.80, 139.49, 140.70, 141.42, 141.80, 142.95, 159.72 (Ar-C), 162.68, 164.30, 178.96 (C=O).

3.2.2.27. *8-(4-Anisyl)-3-methyl-2-(4-nitrophenyl)-6-oxo- N^4, N^5 -diphenyl-2,6-dihydrocinnoline-4,5-dicarboxamide (4l)*. Orange crystals, Lit.⁶⁸ mp 248–250 °C; ^1H NMR (DMSO- d_6): $\delta = 2.35$ (s, 3H, CH_3), 3.78 (s, 3H, OCH_3), 6.92–7.02 (m, 5H, Ar-H), 7.13 (t, $J = 7.8$ Hz, 2H, Ar-H), 7.22–7.31 (m, 4H, Ar-H), 7.47 (m, 2H, Ar-H), 7.54–7.58 (m, 3H, Ar-H), 7.89 (t, $J = 7.8$ Hz, 1H, Ar-H), 8.01 (s, 1H, Ar-H), 8.36 (d, $J = 7.8$ Hz, 1H, Ar-H), 10.40 (br. s, 1H, NH), 10.64 (s, 1H, NH); ^{13}C NMR (DMSO- d_6): $\delta = 19.39$ (CH_3), 55.19 (OCH_3), 113.40, 113.61, 119.43, 119.52, 119.78, 119.93, 122.46, 122.69, 123.59, 123.54, 126.68, 127.54, 128.07, 128.10, 128.32, 128.41, 128.73, 130.91, 131.52, 131.94, 134.53, 134.85, 135.37, 138.63, 139.54, 141.43, 141.95, 142.95, 144.05, 159.58, 159.64 (Ar-C), 162.20, 164.64, 179.15 (C=O).

3.2.2.28. *2-(4-Chlorophenyl)-3-methyl-6-oxo- N^4, N^5 ,8-triphenyl-2,6-dihydrocinnoline-4,5-dicarboxamide (4m)*. Yellow crystals, Lit.⁶⁸ mp 270–271 °C; ^1H NMR (DMSO- d_6): $\delta = 2.36$ (s, 3H, CH_3); 6.97 (t, $J = 7.2$ Hz, 1H, Ar-H), 7.07–7.15 (m, 2H, Ar-H), 7.13 (t, $J = 7.8$ Hz, 2H, Ar-H), 7.25 (t, $J = 8.1$ Hz, 2H, Ar-H), 7.42–7.49 (m, 5H, Ar-H), 7.56 (d, $J = 7.8$ Hz, 2H, Ar-H), 7.65 (d, $J = 8.4$ Hz, 2H, Ar-H), 7.63–7.72 (m, 4H, Ar-H), 10.48 (s, 1H, NH), 10.56 (s, 1H, NH); ^{13}C NMR (DMSO- d_6): $\delta = 19.33$ (CH_3), 115.41, 119.49, 119.79, 122.54, 123.53, 123.95, 127.23, 127.92, 127.98, 128.11, 128.39, 128.59, 129.79, 130.11, 134.49, 135.23, 135.58, 138.75, 139.47, 140.59, 141.32, 141.59, 143.32 (Ar-C), 162.55, 164.23, 178.80 (C=O).

3.2.2.29. *2-(4-Bromophenyl)-3-methyl-6-oxo- N^4, N^5 ,8-triphenyl-2,6-dihydrocinnoline-4,5-dicarboxamide (4n)*. Orange crystals, mp 233–235 °C; IR (KBr): ν/cm^{-1} 3266 (NH), 1677, 1657 (C=O); ^1H NMR (DMSO- d_6): $\delta = 2.35$ (s, 3H, CH_3), 6.97 (t, $J = 7.32$ Hz, 1H, Ar-H), 7.06–7.15 (m, 4H, Ar-H), 7.25 (t, $J = 7.8$ Hz, 2H, Ar-H), 7.42–7.49 (m, 5H, Ar-H), 7.56–7.66 (m, 6H, Ar-H), 7.84–7.86 (m, 2H, Ar-H), 10.46 (s, 1H, NH), 10.55 (s, 1H, NH); ^{13}C NMR (DMSO- d_6): $\delta = 19.33$ (CH_3), 115.43, 119.48, 119.77, 122.52, 123.07, 123.52, 123.93, 127.19, 127.97, 128.09, 128.15, 128.38, 128.57, 130.09, 132.73, 135.21, 135.56, 138.74, 139.46, 140.58, 141.51, 141.73 (Ar-C) 162.58, 164.22, 178.78 (C=O). MS (EI): 627.03 $[\text{M} - 1]^+$. HRMS: calcd for $\text{C}_{35}\text{H}_{25}\text{BrN}_4\text{O}_3$: 628.1110, found 630.1083.

3.2.2.30. *3-Methyl-2-(2-nitrophenyl)-6-oxo- N^4, N^5 ,8-triphenyl-2,6-dihydrocinnoline-4,5-dicarboxamide (4o)*. Orange crystals, mp 251–252 °C; IR (KBr): ν/cm^{-1} 3272 (NH), 1661, 1633 (C=O); ^1H NMR (DMSO- d_6): $\delta = 2.36$ (s, 3H, CH_3), 6.95–6.96 (m, 1H, Ar-H), 7.03–7.05 (m, 2H, Ar-H), 7.11–7.14 (m, 3H, Ar-H), 7.21–7.26 (m, 2H, Ar-H), 7.46–7.47 (m, 2H, Ar-H), 7.37–7.39 (m, 4H, Ar-H), 7.46–7.47 (m, 2H, Ar-H), 7.53–7.57 (m, 2H, Ar-H), 7.88 (t, $J = 7.86$ Hz, 1H, Ar-H), 8.33 (d, $J = 7.98$ Hz, 1H, Ar-H), 10.28 (br s, 1H, NH), 10.67 (s, 1H, NH); ^{13}C NMR (DMSO- d_6): $\delta = 18.54$ (CH_3), 119.41, 119.50, 119.91, 122.57, 123.60, 127.93, 128.33, 128.60, 130.18, 131.93, 134.81, 135.10, 135.36, 138.63, 139.55, 141.33, 141.83, 143.34, 144.06, 152.64 (Ar-C) 162.14, 163.96,

178.95 (C=O). MS (EI): 593.75 $[\text{M} - 1]^+$, HRMS: calcd for $\text{C}_{35}\text{H}_{25}\text{N}_5\text{O}_5$: 595.1855, found 595.1835.

4. Conclusions

In conclusion, a highly chemoselective synthesis of 4-aryloxy-5-hydroxy-1,1'-biphenyl-4-carboxamide derivatives was carried out employing 1 : 1 molar ratio of 3-oxo-2-arylhydrazonopropanals with acetoacetanilide using the optimized condition; DBU/1,4-dioxane under microwave irradiation. Spectroscopic analyses (IR, ^1H - and ^{13}C -NMR, MS and HRMS) and X-ray single crystals of three model examples were used in characterization of the newly isolated compounds. The photophysical properties of the new products were also investigated to assess their optical behavior. Remarkably, compound **3b** displayed a distinctive emission pattern. It had a bathochromic (red) shift with a maximum emission at 709 nm and a noticeable significant Stokes shift at 237 nm. It is anticipated that the currently reported strategy opens a new research avenue in the field of synthetic organic chemistry.

Conflicts of interest

The authors declare that there is no conflict of interest.

Acknowledgements

This research work was funded by the University of Kuwait, grant number (SC01/21). The RSP unit general facilities of the Faculty of Science GFS supported by research grants GS01/05, GS01/03, GS03/01, GS02/01 and GS03/08 are greatly appreciated.

References

- 1 M. J. Macielag, J. P. Demers, S. A. Fraga-Spano, D. J. Hlasta, S. G. Johnson, R. M. Kanojia, R. K. Russell, Z. Sui, M. A. Weidner-Wells and H. Werblood, Substituted salicylanilides as inhibitors of two-component regulatory systems in bacteria, *J. Med. Chem.*, 1998, **41**, 2939–2945.
- 2 M. Krátký and J. Vinšová, Antifungal activity of salicylanilides and their esters with 4-(trifluoromethyl) benzoic acid, *Molecules*, 2012, **17**, 9426–9442.
- 3 G. Paraskevopoulos, S. Monteiro, R. Vosátka, M. Krátký, L. Navrátilová, F. Trejtnar, J. Stolaříková and J. Vinšová, Novel salicylanilides from 4,5-dihalogenated salicylic acids: Synthesis, antimicrobial activity and cytotoxicity, *Bioorg. Med. Chem.*, 2017, **25**, 1524–1532.
- 4 A. Imramovský, J. Vinšová, J. M. Ferriz, V. Buchta and J. Jampílek, Salicylanilide esters of N-protected amino acids as novel antimicrobial agents, *Bioorg. Med. Chem. Lett.*, 2009, **19**, 348–351.
- 5 R. De La Fuente, N. D. Sonawane, D. Arumainayagam and A. S. Verkman, Small molecules with antimicrobial activity against *E. coli* and *P. aeruginosa* identified by high-throughput screening, *Br. J. Pharmacol.*, 2006, **149**, 551–559.
- 6 M. K. Dahlgren, A. M. Kauppi, I.-M. Olsson, A. Linusson and M. Elofsson, Design, synthesis, and multivariate quantitative



- structure–activity relationship of salicylanilides potent inhibitors of type III secretion in *Yersinia*, *J. Med. Chem.*, 2007, **50**, 6177–6188.
- 7 J. Vinsova, A. Imramovsky, V. Buchta, M. Ceckova, M. Dolezal, F. Staud, J. Jampilek and J. Kaustova, Salicylanilide acetates: Synthesis and antibacterial evaluation, *Molecules*, 2006, **12**, 1–12.
- 8 G. Daidone, D. Raffa, S. Plescia, M. Matera, A. Caruso, V. Leone and M. Amico-Roxas, Synthesis and evaluation of the analgesic and antiinflammatory activities of N-substituted salicylamides, *Farmaco*, 1989, **44**, 465–473.
- 9 K. Waisser, J. Matyk, H. Divišová, P. Husakova, J. Kuneš, V. Klimešová, J. Kaustova, U. Möllmann, H. M. Dahse and M. Miko, The oriented development of antitubercotics: salicylanilides, *Arch. Pharm.*, 2006, **339**, 616–620.
- 10 A. Jurgeit, R. McDowell, S. Moese, E. Meldrum, R. Schwendener and U. F. Greber, Niclosamide is a proton carrier and targets acidic endosomes with broad antiviral effects, *PLoS Pathog.*, 2012, **8**, e1002976.
- 11 Y.-W. Chang, T.-K. Yeh, K.-T. Lin, W.-C. Chen, H.-T. Yao, S.-J. Lan, Y.-S. Wu, H.-P. Hsieh, C.-M. Chen and C.-T. Chen, Pharmacokinetics of anti-SARS-CoV agent niclosamide and its analogs in rats, *J. Food Drug Anal.*, 2006, **14**, 15.
- 12 J. Xu, P.-Y. Shi, H. Li and J. Zhou, Broad spectrum antiviral agent niclosamide and its therapeutic potential, *ACS Infect. Dis.*, 2020, **6**, 909–915.
- 13 Z. Baranyai, M. Krátký, R. Vosátka, E. Szabó, Z. Senoner, S. Dávid, J. Stolaříková, J. Vinšová and S. Bősze, In vitro biological evaluation of new antimycobacterial salicylanilide-tuftsin conjugates, *Eur. J. Med. Chem.*, 2017, **133**, 152–173.
- 14 G. Piccaro, F. Giannoni, P. Filippini, A. Mustazzolu and L. Fattorini, Activities of drug combinations against *Mycobacterium tuberculosis* grown in aerobic and hypoxic acidic conditions, *Antimicrob. Agents Chemother.*, 2013, **57**, 1428–1433.
- 15 M. Krátký, J. Vinšová, E. Novotná, J. Mandíková, V. Wsól, F. Trejtnar, V. Ulmann, J. Stolaříková, S. Fernandes and S. Bhat, Salicylanilide derivatives block *Mycobacterium tuberculosis* through inhibition of isocitrate lyase and methionine aminopeptidase, *Tuberculosis*, 2012, **92**, 434–439.
- 16 W. C. Campbell, The chemotherapy of parasitic infections, *J Parasitol.*, 1986, **72**, 45–61.
- 17 J. Bogan and J. Armour, Anthelmintics for ruminants, *Int. J. Parasit.*, 1987, **17**, 483–491.
- 18 R. Rajamuthiah, B. B. Fuchs, E. Jayamani, Y. Kim, J. Larkins-Ford, A. Conery, F. M. Ausubel and E. Mylonakis, Whole animal automated platform for drug discovery against multi-drug resistant *Staphylococcus aureus*, *PLoS One*, 2014, **9**, e89189.
- 19 R. Rajamuthiah, B. B. Fuchs, A. L. Conery, W. Kim, E. Jayamani, B. Kwon, F. M. Ausubel and E. Mylonakis, Repurposing salicylanilide anthelmintic drugs to combat drug resistant *Staphylococcus aureus*, *PLoS One*, 2015, **10**, e0124595.
- 20 H. Mohammad, A. AbdelKhalek, N. S. Abutaleb and M. N. Seleem, Repurposing niclosamide for intestinal decolonization of vancomycin-resistant enterococci, *Int. J. Antimicrob. Agents*, 2018, **51**, 897–904.
- 21 I. E. Escobar, A. White, W. Kim and E. Mylonakis, New antimicrobial bioactivity against multidrug-resistant gram-positive bacteria of kinase inhibitor IMD0354, *Antibiotics*, 2020, **9**, 665.
- 22 V. Srivastava, B. Singh and V. Deorani, Cestodical activity of some compounds against echinococcosis in dogs, *Indian Vet. J.*, 1989, **66**, 807–809.
- 23 Z. Wang, J. Ren, J. Du, H. Wang, J. Liu and G. Wang, Niclosamide as a Promising Therapeutic Player in Human Cancer and Other Diseases, *Int. J. Mol. Sci.*, 2022, **23**, 16116.
- 24 W. Chen, R. A. Mook Jr, R. T. Premont and J. Wang, Niclosamide: Beyond an antihelminthic drug, *Cell. Signalling*, 2018, **41**, 89–96.
- 25 K. Shamim, M. Xu, X. Hu, E. M. Lee, X. Lu, R. Huang, P. Shah, X. Xu, C. Z. Chen, M. Shen, H. Guo, L. Chen, Z. Itkin, R. T. Eastman, P. Shinn, C. Klumpp-Thomas, S. Michael, A. Simeonov, D. C. Lo, G.-l. Ming, H. Song, H. Tang, W. Zheng and W. Huang, Application of niclosamide and analogs as small molecule inhibitors of Zika virus and SARS-CoV-2 infection, *Bioorg. Med. Chem. Lett.*, 2021, **40**, 127906.
- 26 Y.-W. Chang, T. K. Yeh, K.-T. Lin, W.-C. Chen, H.-T. Yao, S. J. Lan, Y.-S. Wu, H. P. Hsieh, C.-m. Chen and C. T. Chen, Pharmacokinetics of anti-SARS-CoV agent niclosamide and its analogs in rats, *J. Food Drug Anal.*, 2006, **14**, 329–333.
- 27 J. Xu, P. Y. Shi, H. Li and J. Zhou, Broad Spectrum Antiviral Agent Niclosamide and Its Therapeutic Potential, *ACS Infect. Dis.*, 2020, **6**, 909–915.
- 28 N. C. Gassen, D. Niemeyer, D. Muth, V. M. Corman, S. Martinelli, A. Gassen, K. Hafner, J. Papies, K. Mösbauer, A. Zellner, A. S. Zannas, A. Herrmann, F. Holsboer, R. Brack-Werner, M. Boshart, B. Müller-Myhsok, C. Drosten, M. A. Müller and T. Rein, SKP2 attenuates autophagy through Beclin1-ubiquitination and its inhibition reduces MERS-Coronavirus infection, *Nat. Commun.*, 2019, **10**, 5770.
- 29 T. Osada, M. Chen, X. Y. Yang, I. Spasojevic, J. B. Vandeusen, D. Hsu, B. M. Clary, T. M. Clay, W. Chen, M. A. Morse and H. K. Lyerly, Antihelminth compound niclosamide downregulates Wnt signaling and elicits antitumor responses in tumors with activating APC mutations, *Cancer Res.*, 2011, **71**, 4172–4182.
- 30 U. Sack, W. Walther, D. Scudiero, M. Selby, D. Kobelt, M. Lemm, I. Fichtner, P. M. Schlag, R. H. Shoemaker and U. Stein, Novel effect of antihelminthic Niclosamide on S100A4-mediated metastatic progression in colon cancer, *J. Natl. Cancer Inst.*, 2011, **103**, 1018–1036.
- 31 Y. Li, P. K. Li, M. J. Roberts, R. C. Arend, R. S. Samant and D. J. Buchsbaum, Multi-targeted therapy of cancer by niclosamide: A new application for an old drug, *Cancer Lett.*, 2014, **349**, 8–14.



- 32 R. A. Mook Jr, J. Wang, X. R. Ren, M. Chen, I. Spasojevic, L. S. Barak, H. K. Lyerly and W. Chen, Structure-activity studies of Wnt/ β -catenin inhibition in the Niclosamide chemotype: Identification of derivatives with improved drug exposure, *Bioorg. Med. Chem.*, 2015, **23**, 5829–5838.
- 33 A. F. Bekhli, M. B. Braude, Z. G. Vorob'eva and V. I. Shvedova, [Synthesis of phenasal], *Med. Prom-st. SSSR*, 1965, **19**, 25–27.
- 34 E. Schraufstätter, W. Meiser and R. Gönnert, Untersuchungen über ein neues Molluscid, *Z. Naturforsch.*, 1961, **16b**, 95–108.
- 35 J. Lal, G. Kaul, A. Akhira, S. B. Ansari, S. Chopra and D. N. Reddy, Bio-evaluation of fluoro and trifluoromethyl-substituted salicylanilides against multidrug-resistant *S. aureus*, *Med. Chem. Res.*, 2021, **30**, 2301–2315.
- 36 A. Fomovska, R. D. Wood, E. Mui, J. P. Dubey, L. R. Ferreira, M. R. Hickman, P. J. Lee, S. Leed, E. Leed, J. M. Auschwitz, W. J. Welsh, C. Sommerville, S. Woods, C. Roberts and R. McLeod, Salicylanilide Inhibitors of *Toxoplasma gondii*, *J. Med. Chem.*, 2012, **55**, 8375–8391.
- 37 A. Kumar, B. Narasimhan and D. Kumar, Synthesis, antimicrobial, and QSAR studies of substituted benzamides, *Bioorg. Med. Chem.*, 2007, **15**, 4113–4124.
- 38 Z.-W. Zhu, L. Shi, X.-M. Ruan, Y. Yang, H.-Q. Li, S.-P. Xu and H.-L. Zhu, Synthesis and antiproliferative activities against Hep-G2 of salicylanilide derivatives: potent inhibitors of the epidermal growth factor receptor (EGFR) tyrosine kinase, *J. Enzyme Inhib. Med. Chem.*, 2011, **26**, 37–45.
- 39 X. Bao and Y. Zhou, Synthesis and recognition properties of a class of simple colorimetric anion chemosensors containing OH and CONH groups, *Sens. Actuators, B*, 2010, **147**, 434–441.
- 40 E. Aki-Sener, K. Bingol, I. Oren, O. Temiz-Arpaci, I. Yalcin and N. Alatanlar, Synthesis and microbiological activity of some N-(o-hydroxyphenyl) benzamides and phenylacetamides as the possible metabolites of antimicrobial active benzoxazoles: part II, *Farmaco*, 2000, **55**, 469–476.
- 41 D. M. Stout, W. Matier, C. Barcelon-Yang, R. D. Reynolds and B. S. Brown, Synthesis and antiarrhythmic and parasympatholytic properties of substituted phenols. 3. Modifications to the linkage region (region 3), *J. Med. Chem.*, 1985, **28**, 295–298.
- 42 M. Gargantilla, L. Persoons, T. Kauerová, N. Del Río, D. Daelemans, E.-M. Priego, P. Kollar and M.-J. Pérez-Pérez, Hybridization Approach to Identify Salicylanilides as Inhibitors of Tubulin Polymerization and Signal Transducers and Activators of Transcription 3 (STAT3), *Pharmaceuticals*, 2022, **15**, 835.
- 43 A. Islam, I. Hannout, E. Hassan and A. Ihsan, Synthesis of some substituted salicylanilides of expected biological activity, *J. Prakt. Chem./Chem.-Ztg.*, 1972, **314**, 727–734.
- 44 K. Hunger, *Industrial dyes: chemistry, properties, applications*, John Wiley & Sons, 2007.
- 45 Y. Zhao and T. Ikeda, *Smart light-responsive materials: azobenzene-containing polymers and liquid crystals*, John Wiley & Sons, 2009.
- 46 L. W. Giles, J. B. Marlow, C. S. Butler, G. A. Turpin, L. De Campo, S. T. Mudie, C. F. Faul and R. F. Tabor, Structural relationships for the design of responsive azobenzene-based lyotropic liquid crystals, *Phys. Chem. Chem. Phys.*, 2020, **22**, 4086–4095.
- 47 F. A. Pennacchio, C. Fedele, S. De Martino, S. Cavalli, R. Vecchione and P. A. Netti, Three-dimensional microstructured azobenzene-containing gelatin as a photoactuable cell confining system, *ACS Appl. Mater. Interfaces*, 2018, **10**, 91–97.
- 48 J. García-Amorós and D. Velasco, Recent advances towards azobenzene-based light-driven real-time information-transmitting materials, *Beilstein J. Org. Chem.*, 2012, **8**, 1003–1017.
- 49 N. DiCesare and J. R. Lakowicz, New color chemosensors for monosaccharides based on Azo dyes, *Org. Lett.*, 2001, **3**, 3891–3893.
- 50 K. C. Chang, I. H. Su, Y. Y. Wang and W. S. Chung, A bifunctional chromogenic calix [4] arene chemosensor for both cations and anions: a potential Ca^{2+} and F^- switched INHIBIT logic gate with a YES logic function, *Eur. J. Org. Chem.*, 2010, **24**, 4700–4704.
- 51 F. Puntoriero, P. Ceroni, V. Balzani, G. Bergamini and F. Vögtle, Photoswitchable dendritic hosts: a dendrimer with peripheral azobenzene groups, *J. Am. Chem. Soc.*, 2007, **129**, 10714–10719.
- 52 V. Ferri, M. Elbing, G. Pace, M. D. Dickey, M. Zharnikov, P. Samori, M. Mayor and M. A. Rampi, Light-powered electrical switch based on cargo-lifting azobenzene monolayers, *Angew. Chem., Int. Ed.*, 2008, **120**, 3455–3457.
- 53 J. S. Carey, D. Laffan, C. Thomson and M. T. Williams, Analysis of the reactions used for the preparation of drug candidate molecules, *Org. Biomol. Chem.*, 2006, **4**, 2337–2347.
- 54 S. D. Roughley and A. M. Jordan, The medicinal chemist's toolbox: an analysis of reactions used in the pursuit of drug candidates, *J. Med. Chem.*, 2011, **54**, 3451–3479.
- 55 S.-P. Wang, C. W. Cheung and J.-A. Ma, Direct amidation of carboxylic acids with nitroarenes, *J. Org. Chem.*, 2019, **84**, 13922–13934.
- 56 B. K. Banik and D. Bandyopadhyay, *Advances in Microwave Chemistry*, CRC Press, 2018.
- 57 S. C. Ameta, P. B. Punjabi, R. Ameta and C. Ameta, *Microwave-assisted organic synthesis: a green chemical approach*, CRC Press, 2014.
- 58 D. Bogdal, *Microwave-assisted organic synthesis: one hundred reaction procedures*, Elsevier, 2005.
- 59 L. Perreux, A. Loupy and F. Volatron, Solvent-free preparation of amides from acids and primary amines under microwave irradiation, *Tetrahedron*, 2002, **58**, 2155–2162.
- 60 E. Gelens, L. Smeets, L. A. Sliedregt, B. J. van Steen, C. G. Kruse, R. Leurs and R. V. Orru, An atom efficient and solvent-free synthesis of structurally diverse amides using microwaves, *Tetrahedron Lett.*, 2005, **46**, 3751–3754.
- 61 A. Khalafi-Nezhad, A. Parhami, M. N. S. Rad and A. Zarea, Efficient method for the direct preparation of amides from



- carboxylic acids using tosyl chloride under solvent-free conditions, *Tetrahedron Lett.*, 2005, **46**, 6879–6882.
- 62 R. R. Poondra and N. J. Turner, Microwave-assisted sequential amide bond formation and intramolecular amidation: a rapid entry to functionalized oxindoles, *Org. Lett.*, 2005, **7**, 863–866.
- 63 C. Ferroud, M. Godart, S. Ung, H. Borderies and A. Guy, Microwaves-assisted solvent-free synthesis of N-acetamides by amidation or aminolysis, *Tetrahedron Lett.*, 2008, **49**, 3004–3008.
- 64 M. P. Vázquez-Tato, Microwave-mediated synthesis of amides, *Synlett*, 1993, **7**, 506.
- 65 G. Paraskevopoulos, M. Krátký, J. Mandíková, F. Trejtnar, J. Stolaříková, P. Pávek, G. Besra and J. Vinšová, Novel derivatives of nitro-substituted salicylic acids: Synthesis, antimicrobial activity and cytotoxicity, *Bioorg. Med. Chem.*, 2015, **23**, 7292–7301.
- 66 A. M. Alazemi, K. M. Dawood, H. M. Al-Matar and W. M. Tohamy, Efficient and Recyclable Solid-Supported Pd(II) Catalyst for Microwave-Assisted Suzuki Cross-Coupling in Aqueous Medium, *ACS Omega*, 2022, **7**, 28831–28848.
- 67 H. M. Al-Matar, K. M. Dawood, W. M. Tohamy and M. A. Shalaby, Facile Assembling of Novel 2,3,6,7,9-pentaazabicyclo-[3.3.1] nona-3,7-diene Derivatives under Microwave and Ultrasound Platforms, *Molecules*, 2019, **24**, 1110.
- 68 H. M. Al-Matar, K. M. Dawood and W. M. Tohamy, Tandem one-pot synthesis of 2-arylcinolin-6-one derivatives from arylhydrazonopropanals and acetoacetanilides using sustainable ultrasound and microwave platforms, *RSC Adv.*, 2018, **8**, 34459–34467.
- 69 K. M. Dawood and M. Alaasar, Transition-metal-catalyzed Heteroannulation Reactions in Aqueous Medium, *Asian J. Org. Chem.*, 2022, **11**, e202200331.
- 70 K. M. Dawood, Microwave-assisted Suzuki–Miyaura and Heck–Mizoroki cross-coupling reactions of aryl chlorides and bromides in water using stable benzothiazole-based palladium(II) precatalysts, *Tetrahedron*, 2007, **63**, 9642–9651.
- 71 K. M. Dawood, M. B. Elamin and A. M. Farag, Microwave-Assisted Synthesis of Arylated Pyrrolo [2,1-a] Isoquinoline Derivatives via Sequential [3 + 2] Cycloadditions and Suzuki–Miyaura Cross-Couplings in Aqueous Medium, *J. Heterocycl. Chem.*, 2016, **53**, 1928–1934.
- 72 K. M. Dawood and M. M. El-Deftar, Microwave-assisted CC cross-coupling reactions of aryl and heteroaryl halides in water, *Arkivoc*, 2010, **9**, 319–330.
- 73 K. M. Dawood and M. M. El-Deftar, Microwave-assisted synthesis of 2-substituted 4-biaryl-1,3-thiazoles by carbon-carbon cross-coupling in water, *Synthesis*, 2010, **6**, 1030–1038.
- 74 K. M. Dawood and A. Kirschning, Combining enabling techniques in organic synthesis: solid-phase-assisted catalysis under microwave conditions using a stable Pd(II)-precatalyst, *Tetrahedron*, 2005, **61**, 12121–12130.
- 75 K. M. Dawood, W. Solodenko and A. Kirschning, Microwave-accelerated Mizoroki–Heck and Sonogashira cross-coupling reactions in water using a heterogeneous palladium(II)-precatalyst, *Arkivoc*, 2007, **7**, 104–124.
- 76 K. M. Dawood, M. B. Elamin and A. M. Farag, Microwave-assisted synthesis of 2-acetyl-5-arylthiophenes and 4-(5-arylthiophen-2-yl) thiazoles via Suzuki coupling in water, *Arkivoc*, 2015, **7**, 50–62.
- 77 K. M. Dawood, A. M. Farag, M. M. El-Deftar, M. Gardiner and H. A. Abdelaziz, Microwave-assisted synthesis of 5-arylbenzofuran-2-carboxylates via Suzuki coupling using a 2-quinolinealldoxime-Pd(II)-complex, *Arkivoc*, 2013, **3**, 210–226.
- 78 M. A. Al-Shiekh, H. Y. Medrassi, M. H. Elnagdi and E. A. Hafez, Substituted hydrazonals as building blocks in heterocyclic synthesis: A new route to arylhydrazonocinnolines, *J. Chem. Res.*, 2007, **7**, 432–436.
- 79 H. M. Hassaneen and I. A. Abdelhamid, Acetylacetaldehyde Dimethyl Acetal as Versatile Precursors for the Synthesis of Arylazonicotinic Acid Derivatives: Green Multicomponent Syntheses of Bioactive Poly-Heteroaromatic Compounds, *J. Heterocycl. Chem.*, 2017, **54**, 1048–1053.
- 80 The Crystallographic Data for compounds **3f** (ref. CCDC 2270147), **3h** (ref. CCDC 2270148), and **3n** (ref. CCDC 2270149†).
- 81 J. R. Lakowicz, *Principles of fluorescence spectroscopy*, Springer, 2006.
- 82 J. Zhao, S. Ji, Y. Chen, H. Guo and P. Yang, Excited state intramolecular proton transfer (ESIPT): from principal photophysics to the development of new chromophores and applications in fluorescent molecular probes and luminescent materials, *Phys. Chem. Chem. Phys.*, 2012, **14**, 8803–8817.

